

# 6. Analytical Studies

## 6.1 Overview

Analytical studies were conducted as part of this project to serve two broad objectives: (1) to assess the effects of damage from a prior earthquake on the response of single-degree-of-freedom oscillators to a subsequent, hypothetical performance-level earthquake, and (2) to evaluate the utility of simple, design-oriented methods for estimating the response of damaged structures. Previous analytical studies were also reviewed.

To assess the effects of prior damage on response to a performance-level earthquake, damage to a large number of single-degree-of-freedom (SDOF) oscillators was simulated. The initially “damaged” oscillators were then subjected to an assortment of ground motions. The response of the damaged oscillators was compared with that of their undamaged counterparts to identify how the damage affected the response.

The oscillators ranged in initial period from 0.1 to 2.0 seconds, and the strength values were specified such that the oscillators achieved displacement ductility values of 1, 2, 4, and 8 for each of the ground motions when using a bilinear force-displacement model. The effects of damage were computed for these oscillators using several Takeda-based force-displacement models. Damage was parameterized independently in terms of ductility demand and strength reduction.

Ground motions were selected to represent a broad range of frequency characteristics in each of the following categories: Short-duration (SD) records were selected from earthquakes with magnitudes less than about 7, while long-duration (LD) records were generally selected from stronger earthquakes. A third category, forward directivity (FD), consists of ground motions recorded near the fault rupture surface for which a strong velocity pulse may be observed very early in the S-wave portion of the record. Six motions were selected for each category, representing different frequency characteristics, source mechanisms, and earthquakes occurring in locations around the world over the last half-century.

The utility of simple, design-oriented methods for estimating response was evaluated for the damaged and undamaged SDOF oscillators. The displacement coefficient method is presented in FEMA 273 (FEMA, 1997a) and the capacity spectrum and secant stiffness

methods is presented in ATC-40 (ATC, 1996). Estimates of peak displacement response were determined according to these methods and compared with computed values obtained in the dynamic analyses for the damaged and undamaged structures. In addition, the ratio of the peak displacement estimates of damaged and undamaged structures was compared with the ratio obtained from the displacements computed in the nonlinear dynamic analyses.

This chapter summarizes related findings by previous investigators in Section 6.2. The dynamic analysis framework is described in detail in Section 6.3, and results of the nonlinear dynamic analyses are presented in Section 6.4. The design-oriented nonlinear static procedures are described in Section 6.5, and the results of these analyses are compared with the results computed in the dynamic analyses in Section 6.6. Conclusions and implications of the work are presented in Section 6.7.

## 6.2 Summary of Previous Findings

Previous studies have addressed several issues related to this project. Relevant analytical and experimental findings are reviewed in this section.

### 6.2.1 Hysteresis Models

Studies of response to recorded ground motions have used many force-displacement models that incorporate various rules for modeling hysteretic response. By far, the most common of these are the bilinear and stiffness-degrading models, which repeatedly attain the strengths given by the monotonic or envelope force-displacement relation. The response of oscillators modeled using bilinear or stiffness-degrading models is discussed below.

#### 6.2.1.1 Bilinear and Stiffness-Degrading Models

Many studies (for example, Iwan, 1977; Newmark and Riddell, 1979; Riddell, 1980; Humar, 1980; Fajfar and Fischinger, 1984; Shimazaki and Sozen, 1984; and Minami and Osawa, 1988) have examined the effect of the hysteresis model on the response of SDOF structures. These studies considered elastic-perfectly-plastic, bilinear (with positive post-yield stiffness), and stiffness-degrading models such as the Takeda model

and the Q model, as well as some lesser-known models. For the nonlinear models used in these studies, the post-yield stiffness of the primary curve ranged between 0 and 10% of the initial stiffness. It is generally found that for long-period structures with positive post-yield stiffness, peak displacement response tends to be independent of the hysteresis model, and it is approximately equal to the peak displacement of linear-elastic oscillators having the same initial stiffness. For shorter-period structures, however, peak displacement response tends to exceed the response of linear-elastic oscillators having the same initial stiffness. The difference in displacement response is exacerbated in lower-strength oscillators. Fajfar and Fischinger (1984), found that for shorter-period oscillators, the peak displacements of elastic-perfectly-plastic models tend to exceed those of degrading-stiffness models (the Q-model), and these peak displacements tend to exceed those of the bilinear model. Riddell (1980), reported that the response of stiffness-degrading systems tends to “go below the peaks and above the troughs” of the spectra obtained for elastoplastic systems.

The dynamic response of reinforced concrete structures tested on laboratory shake tables has been compared with the response computed using different hysteretic models. The Takeda model was shown to give good agreement with measured response characteristics (Takeda et al., 1970). In a subsequent study, the Takeda model was shown to match closely the recorded response; acceptable results were obtained with the less-complicated Q-Hyst model (Saiidi, 1980). Time histories computed by these models were far more accurate than those obtained with the bilinear model.

Studies of a seven-story reinforced concrete moment-resisting frame building damaged in the 1994 Northridge earthquake yield similar conclusions. Moehle et al. (1997) reported that the response computed for plane-frame representations of the structure most nearly matched the recorded response when the frame members were modeled using stiffness-degrading models and strength- and stiffness-degrading force/displacement relationships; dynamic analysis results obtained using bilinear force/displacement relationships were not sufficiently accurate.

Iwan (1973) examined the effect of pinching and yielding on the response of SDOF oscillators to four records. It was found that the maximum displacement response of oscillators having an initial period equal to one second was very nearly equal to that computed for

bilinear systems having the same initial stiffness and yield strength. For one-second oscillators having different system parameters and subjected to different earthquake records, the ratio of mean degrading-system peak displacement response to bilinear system response was 1.06, with standard deviation of 0.14. Iwan noted that for periods appreciably less than one second, the response of degrading systems was significantly greater than that for the corresponding bilinear system, but these effects were not quantified.

Iwan (1977) reported on the effects of a reduction in stiffness caused by cracking. Modeling the uncracked stiffness caused a reduction in peak displacement response for shorter-period oscillators with displacement ductility values less than four, when compared with the response of systems having initial stiffness equal to the yield-point secant stiffness.

Humar (1980) compared the displacement ductility demand calculated for the bilinear and Takeda models for SDOF and multi-degree-of-freedom (MDOF) systems. For the shorter-period SDOF oscillators, the displacement ductility demands exceeded the strength-reduction factor, particularly for the Takeda model. Five- and ten-story frames were designed with girder strengths set equal to 25% of the demands computed in an elastic analysis, and column strengths were set higher than the values computed in an elastic analysis. The Takeda model, which included stiffness degradation, generally led to larger interstory drifts and girder ductility demands than were computed with the bilinear model.

The studies described above considered hysteretic models for which the slope of the post-yield portion of the primary curve was greater than or equal to zero. Where negative post-yield slopes are present, peak displacement response is heightened (Mahin, 1980). The change in peak displacement response tends to be significantly larger for decreases in the post-yield slope below zero than for similar increases above zero. Even post-yield stiffness values equal to negative 1% of the yield stiffness were sufficient to cause collapse. These effects were found to be more pronounced in shorter-period systems and in relatively weak systems.

Rahnama and Krawinkler (1995) reported findings for SDOF structures subjected to 15 records obtained on rock sites. They found that higher lateral strength is required, relative to elastic demands to obtain target displacement ductility demands, for oscillators with

negative post-yield stiffness. The decrease in the strength-reduction factor is relatively independent of vibration period and is more dramatic with increases in target displacement ductility demand. These effects depend on the hysteresis model; the effect of negative post-yield stiffness on the strength-reduction factor is much smaller for stiffness-degrading systems than for bilinear systems. They note that stiffness-degrading systems behave similarly to bilinear systems for positive post-yield stiffness, and they are clearly superior to systems with negative values of post-yield stiffness.

Palazzo and DeLuca (1984) found that the strength required to avoid collapse of SDOF oscillators subjected to the Irpinia earthquake increased as the post-yield stiffness of the oscillator became increasingly negative. Xie and Zhang (1988) compared the response of stiffness-degrading models (having zero post-yield stiffness) with the response of models having a negative post-yield stiffness. The SDOF oscillators were subjected to 40 synthetic records having duration varying from 6 to 30 seconds. It appears that Xie and Zhang found that for shorter-period structures, negative post-yield stiffness models were more likely to result in collapse than were the stiffness-degrading models for all durations considered.

### 6.2.1.2 Strength-Degrading Models

The response of structures for which the attainable strength is reduced with repeated cyclic loading is discussed below.

Parducci and Mezzi (1984) used elasto-plastic force-displacement models to examine the effects of strength degradation. Yield strength was modeled as decreasing linearly with cumulative plastic deformation. Using accelerograms recorded in Italian earthquakes, The authors found that strength degradation causes an increase in displacement ductility demand for the stronger, shorter-period oscillators. For weaker oscillators, strength degradation amplifies ductility demand over a broader range of periods. The more rapid the degradation of strength, the greater the increase in ductility demand. An analogy can be made with the findings of Shimazaki and Sozen (1984): when strength degradation occurs, the increase in ductility demand can be kept small for shorter-period structures if sufficient strength is provided.

Nakamura and Tanida (1988) examined the effect of strength degradation and slip on the response of SDOF oscillators to white noise and to the 1940 NS El Centro motion. Figure 6-1 plots the force/displacement response curves obtained in this study for various combinations of hysteresis parameters for oscillators with a 0.2-sec period. The parameter  $D$  controls the

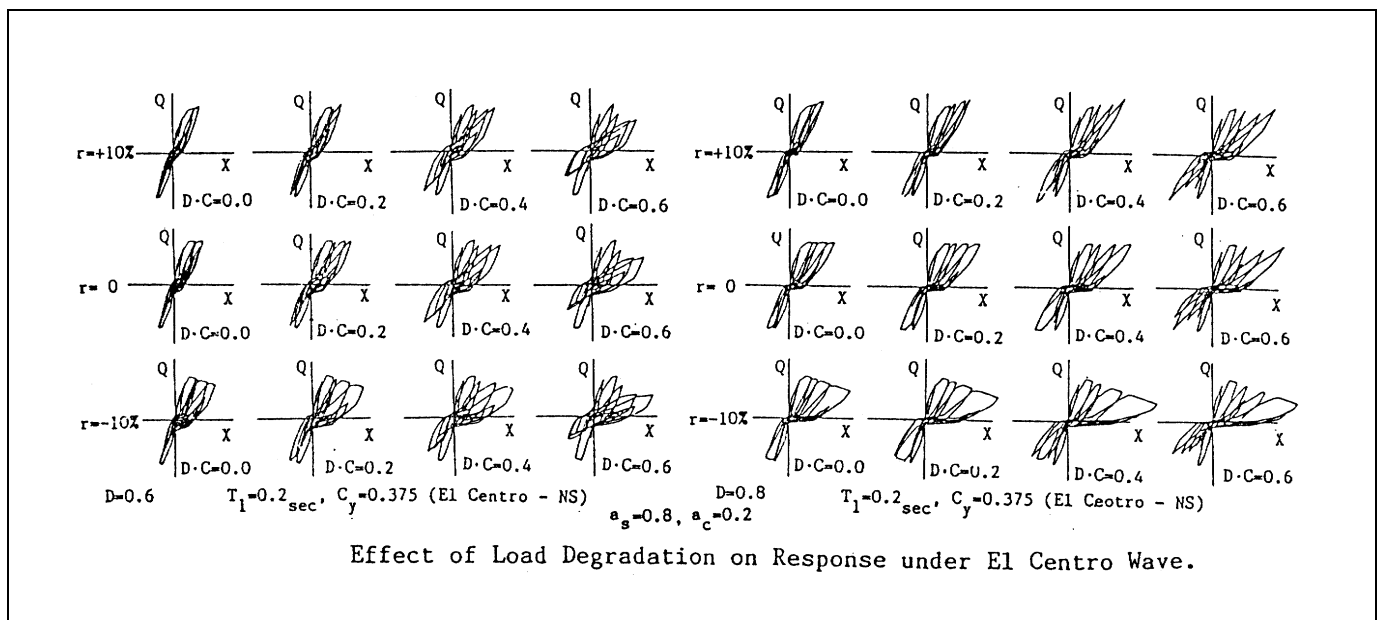


Figure 6-1 Effect of Hysteretic Properties on Response to 1940 NS El Centro Record (from Nakamura, 1988)

amount of slip,  $C$  controls the degraded loading stiffness, and  $a_s$  and  $a_c$  control the unloading stiffness for the slip and degrading components of the model. It is clear that peak displacement response tends to increase as slip becomes more prominent, as post-yield stiffness decreases or even becomes negative, and as loading stiffness decreases.

Rahnama and Krawinkler (1995) modeled strength degradation for SDOF systems as a function of dissipated hysteretic energy. Strength degradation may greatly affect the response of SDOF systems, and the response is sensitive to the choice of parameters by which the strength degradation is modeled. Results of such studies need to be tied to realistic degradation relationships to understand the practical significance of computed results.

### **6.2.2 Effect of Ground Motion Duration**

As described previously, Xie and Zhang (1988) subjected a number of SDOF oscillators to 40 synthetic ground motions, which lasted from 6 to 30 seconds. For stiffness-degrading and negative post-yield stiffness models, the number of collapses increased, as ground motion duration increased. The incidence of collapse tended to be higher for shorter-period structures than longer-period structures. Shorter-duration ground motions that were just sufficient to trigger the collapse of short-period structures did not trigger the collapse of any longer-period structures.

Mahin (1980) reported on the evolution of ductility demand with time for SDOF oscillators subjected to five synthetic records, each having a 60-second duration. Peak evolutionary ductility demands were plotted at 10-second intervals for bilinear oscillators; ductility demand was found to increase asymptotically toward the peak values obtained at 60 seconds. This implies that increases in the duration of ground motion may cause relatively smaller increases in ductility demand.

Sewell (1992) studied the effect of ground-motion duration on elastic demand, constant-ductility strength-reduction factors, and inelastic response intensity, using a set of 262 ground-motion records. He found that the spectral acceleration of elastic and inelastic systems is not correlated with duration, and that strength-reduction factors can be estimated using elastic response ordinates. These findings suggest that the effect of

duration on inelastic response is contained within representations of elastic response quantities.

### **6.2.3 Residual Displacement**

Kawashima et al. (1994) studied the response of bilinear systems with periods between 0.1 and 3 seconds that were subjected to Japanese ground-motion records. According to this study, residual displacement values are strongly dependent on the post-yield stiffness of the bilinear system; that is, systems with larger post-yield stiffness tend to have significantly smaller residual displacements, and systems with zero or negative post-yield stiffness tend to have residual displacements that approach the peak response displacement. They also found that the magnitude of residual displacement, normalized by peak displacement, tends to be independent of displacement ductility demand, based on displacement ductility demands of two, four, and six. The results also indicated that the magnitude of residual displacement is not strongly dependent on the characteristic period of the ground motion, the magnitude of the earthquake, or the distance from the epicenter.

In shake-table tests of reinforced concrete wall and frame/wall structures, Araki et al. (1990) reported that residual drifts for all tests were less than 0.2% of structure height. These tests included wall structures exhibiting displacement ductility demands up to about 12 and frame/wall structures exhibiting displacement ductility demands up to about 14. The small residual drifts in this study were attributed to the presence of restoring forces (acting on the mass of the structure), which are generated as the wall lengthens when displaced laterally. Typical response analyses do not model these restoring forces. These results appear to be applicable to systems dominated by flexural response. However, larger residual displacements have been observed in postearthquake reconnaissance.

### **6.2.4 Repeated Loading**

In the shake-table tests, Araki et al. (1990) also subjected reinforced concrete wall and frame-wall structures to single and repeated motions. It appears that a synthetic ground motion was used. It was found that the low-rise structures subjected to repeated shake-table tests displaced to approximately twice as much as they did in a single test. For the mid-rise and high-rise structures, repeated testing caused peak displacements that were approximately 0 to 10% larger than those obtained in single tests.

Wolschlag (1993) tested three-story reinforced concrete walls on a shake table. In one test series, an undamaged structure was subjected to repeated ground motions of the same intensity. In the repeat tests, the peak displacement response at each floor of the damaged specimen hardly differed from the response measured for the initially undamaged structure.

Cecen (1979) tested two identical ten-story, three-bay, reinforced concrete frame models on a shake table. The two models were subjected to sequences of base motions of differing intensity, followed by a final test using identical base motions. When the structures were subjected to the repeated base motion, the peak displacement response at each story was only slightly affected by the previous shaking of the same intensity. When the two structures were subjected to the same final motion, peak displacement response over the height of the two structures was only slightly affected by the different prior sequences. Floor acceleration response, however, was prone to more variation.

Mahin (1980) investigated the analytical response of SDOF oscillators to repeated ground motions. He reported minor-to-moderate increases in displacement ductility demand across all periods, and weaker structures were prone to the largest increases. For bilinear models with negative post-yield stiffness, increased duration or repeated ground motions tended to cause significant increases in displacement ductility demand (Mahin and Boroschek, 1991).

## **6.3 Dynamic Analysis Framework**

### **6.3.1 Overview**

This section describes the dynamic analyses determining the effects of damage from prior earthquakes on the response to a subsequent performance-level earthquake. In particular, this section describes the ground motion and hysteresis models, the properties of the undamaged oscillators, and the assumptions and constructions used to establish the initially-damaged oscillators. Results of the dynamic analyses are presented in Section 6.4.

### **6.3.2 Dynamic Analysis Approach**

The aim of dynamic analysis was to quantify the effects of a damaging earthquake on the response of a SDOF oscillator to a subsequent, hypothetical, performance-event earthquake. Two obvious approaches may be

taken: the first simulates the damaging earthquake, and the second simulates the damage caused by the damaging earthquake.

To simulate the damaging earthquake, oscillators can be subjected to an acceleration record that is composed of an initial, damaging ground motion record, a quiescent period, and a final ground motion record specified as the performance-level event. This approach appears to simulate reality well, but it is difficult to determine *a priori* how to specify the intensity of the damaging ground motion. One rationale would be to impose damaging earthquakes that cause specified degrees of ductility demand. This would result in oscillators having experienced prior ductility demand and residual displacement at the start of the performance-level ground motion.

In the second approach, taken in this study, the force-displacement curve of the oscillator is modified prescriptively to simulate prior ductility demand, and these analytically “damaged” oscillators are subjected to only the performance-level ground motion. To identify the effects of damage (through changes in stiffness and strength of the oscillator force/displacement response), the possibility of significant residual displacements resulting from the damaging earthquake was neglected. Thus, the damaging earthquake is considered to have imposed prior ductility demands (PDD), possibly in conjunction with strength reduction or strength degradation, on an initially-undamaged oscillator. Initial stiffness, initial unloading stiffness, and strength of the oscillators at the start of the performance-level ground motion may be affected. Response of the initially-damaged structure is compared with the response of the undamaged structure under the performance-level motion. This approach presumes that an engineer will be able to assess changes in lateral stiffness and strength of a real structure based on the nature of damage observed after the damaging earthquake.

While a number of indices may be used to compare response intensity, peak displacement response is preferred here because of its relative simplicity, its immediate physical significance, and its use as the basic parameter in the nonlinear static procedures (described in Section 6.5). The utility of the nonlinear static procedures is assessed vis-a-vis their ability to estimate accurately the peak displacement response.

It should be recognized that predicting the capacity of wall and infill elements may be difficult and prone to uncertainty, whether indexed by displacement, energy,

or other measures. When various modes of response may contribute significantly to an element's behavior, existing models may not reliably identify which mode will dominate. Uncertainty in the dominant mode necessarily leads to uncertainty in estimates of the various capacity measures.

### 6.3.3 Ground Motions

Several issues were considered when identifying ground motion records to be used in the analyses. First, the relative strength of the oscillators and the duration of ground motion are thought to be significant because these parameters control the prominence of inelastic response. Second, it is known that ground motions rich in frequencies just below the initial frequency of the structure tend to exacerbate damage, because the period of the structure lengthens as yielding progresses. Third, information is needed on the characteristics of structural response to near-field motions having forward-directivity effects.

The analyses were intended to identify possible effects of duration and forward directivity on the response of damaged structures. Therefore, three categories of ground motions were established: short duration (SD), long duration (LD), and Forward Directivity (FD). The characteristics of several hundred ground motions were considered in detail in order to select the records used in each category. Ground motions within a category were selected to represent a broad range of frequency content. In addition, it was desired to use some records that were familiar to the research community, and to use some records obtained from the Loma Prieta, Northridge, and Kobe earthquakes. Within these constraints, records were selected from a diverse worldwide set of earthquakes in order to avoid systematic biases that might otherwise occur. Six time series were used in each category to provide a statistical base on which to interpret response trends and variability. Table 6-1 identifies the ground motions that compose each category, sorted by characteristic period.

Record duration was judged qualitatively in order to sort the records into the short duration and long duration categories. The categorization is intended to discriminate broadly between records for which the duration of inelastic response is short or long. Because the duration of inelastic response depends fundamentally on the oscillator period, the relative strength, and the force/displacement model, a suitable scalar index of record duration is not available.

The physical rupture process tends to correlate ground-motion duration and earthquake magnitude. It can be observed that earthquakes with magnitudes less than 7 tended to produce records that were categorized as short-duration motions, while those with magnitudes greater than 7 tended to be categorized as long-duration motions.

Ground motions recorded near a rupturing fault may contain relatively large velocity pulses if the fault rupture progresses toward the recording station. Motions selected for the forward directivity category were identified by others as containing near-field pulses (Somerville et al., 1997). Recorded components aligned most nearly with the direction perpendicular to the fault trace were selected for this category.

The records shown in Table 6-1 are known to come from damaging earthquakes. The peak ground acceleration values shown in Table 6-1 are in units of the acceleration of gravity. The actual value of peak ground acceleration does not bear directly on the results of this study, because oscillator strength is determined relative to the peak ground acceleration in order to obtain specified displacement ductility demands.

Identifiers in Table 6-1 are formulated using two characters to represent the earthquake, followed by two digits representing the year, followed by four characters representing the recording station, followed by three digits representing the compass bearing of the ground-motion component. Thus, IV40ELCN.180 identifies the South-North component recorded at El Centro in the 1940 Imperial Valley earthquake. Various magnitude measures are reported in the literature and repeated here for reference:  $M_L$  represents the traditional local or Richter magnitude,  $M_W$  represents moment magnitude, and  $M_S$  represents the surface-wave magnitude.

Detailed plots of the ground motions listed in Table 6-1 are presented in Figures 6-2 through 6-19. The plots present ground motion acceleration, velocity, and displacement time-series data, as well as spectral-response quantities. In all cases, ground acceleration data were used in the response computations, assuming zero initial velocity and displacement. For most records, the ground velocity and displacement data presented in the figures were prepared by others. For the four records identified with an asterisk (\*) in Table 6-1, informal integration procedures were used to obtain the ground velocity and displacement values shown.

(Text continued on page 120)

**Chapter 6: Analytical Studies**

**Table 6-1 Recorded Ground Motions Used in the Analyses**

Identifier	Earthquake Date	Mag.	Station	Component	PGA (g)	Epic. Dist. (km)	Char. Period (sec)
<b>Short Duration (SD)</b>							
WN87MWLN.090	Whittier Narrows 1 Oct 87	$M_L=6.1$	Mount Wilson Caltech Seismic Station	90	0.175	18	0.20
BB92CIVC.360	Big Bear 28 Jun 92	$M_s=6.6$	Civic Center Grounds	360	0.544	12	0.40
SP88GUKA.360 *	Spitak 7 Dec 88	$M_s=6.9$	Gukasyan, Armenia	360	0.207	57	0.55
LP89CORR.090	Loma Prieta 17 Oct 89	$M_s=7.1$	Corralitos Eureka Canyon Rd.	90	0.478	8	0.85
NR94CENT.360	Northridge 17 Jan 94	$M_w=6.7$	Century City	360	0.221	19	1.00
IV79ARY7.140	Imperial Valley 15 Oct 79	$M_L=6.6$	Array #7-14	140	0.333	27	1.20
<b>Long Duration (LD)</b>							
CH85LLEO.010	Central Chile 3 Mar 85	$M_s=7.8$	Llolleo-Baseament of 1- Story Building	010	0.711	60	0.30
CH85VALP.070	Central Chile 3 Mar 85	$M_s=7.8$	Valparaiso University of Santa Maria	070	0.176	26	0.55
IV40ELCN.180	Imperial Valley 18 May 40	$M_L=6.3$	El Centro Irrigation District	180	0.348	12	0.65
TB78TABS.344 *	Tabas 16 Sep 78	$M=7.4$	Tabas	344	0.937	<3	0.80
LN92JOSH.360	Landers 28 Jun 92	$M=7.5$	Joshua Tree	360	0.274	15	1.30
MX85SCT1.270	Michoacan 19 Sep 85	$M_s=8.1$	SCT1-Secretary of Com- munication and Transpor- tation	270	0.171	376	2.00
<b>Forward Directivity (FD)</b>							
LN92LUCN.250 *	Landers 28 Jun 92	$M=7.5$	Lucerne	250	0.733	42	0.20
IV79BRWY.315	Imperial Valley 15 Oct 79	$M_L=6.6$	Brawley Municipal Airport	315	0.221	43	0.35
LP89SARA.360	Loma Prieta 17 Oct 89	$M_s=7.1$	Saratoga Aloha Avenue	360	0.504	28	0.40
NR94NWHL.360	Northridge 17 Jan 94	$M_w=6.7$	Newhall LA County Fire Station	360	0.589	19	0.80
NR94SYLH.090	Northridge 17 Jan 94	$M_w=6.7$	Sylmar County Hospital Parking Lot	090	0.604	15	0.90
KO95TTRI.360 *	Hyogo-Ken Nambu 17 Jan 95	$M_L=7.2$	Takatori-kisu	360	0.617	11	1.40
* Indicates that informal integration procedures were used to calculate the velocity and displacement histories shown in Figures 6-2 through 6-19.							

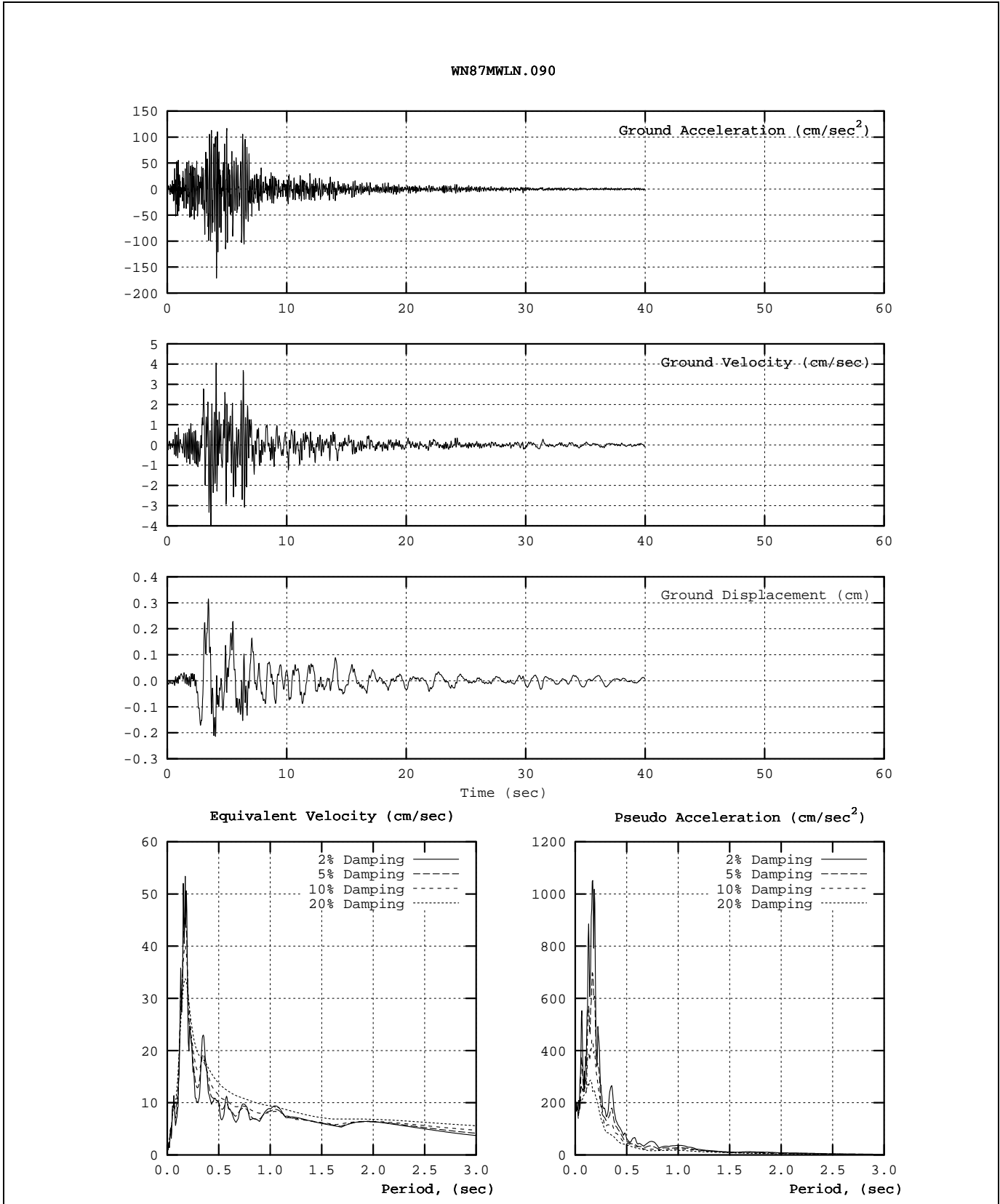


Figure 6-2 Characteristics of the WN87MWLN.090 (Mount Wilson) Ground Motion

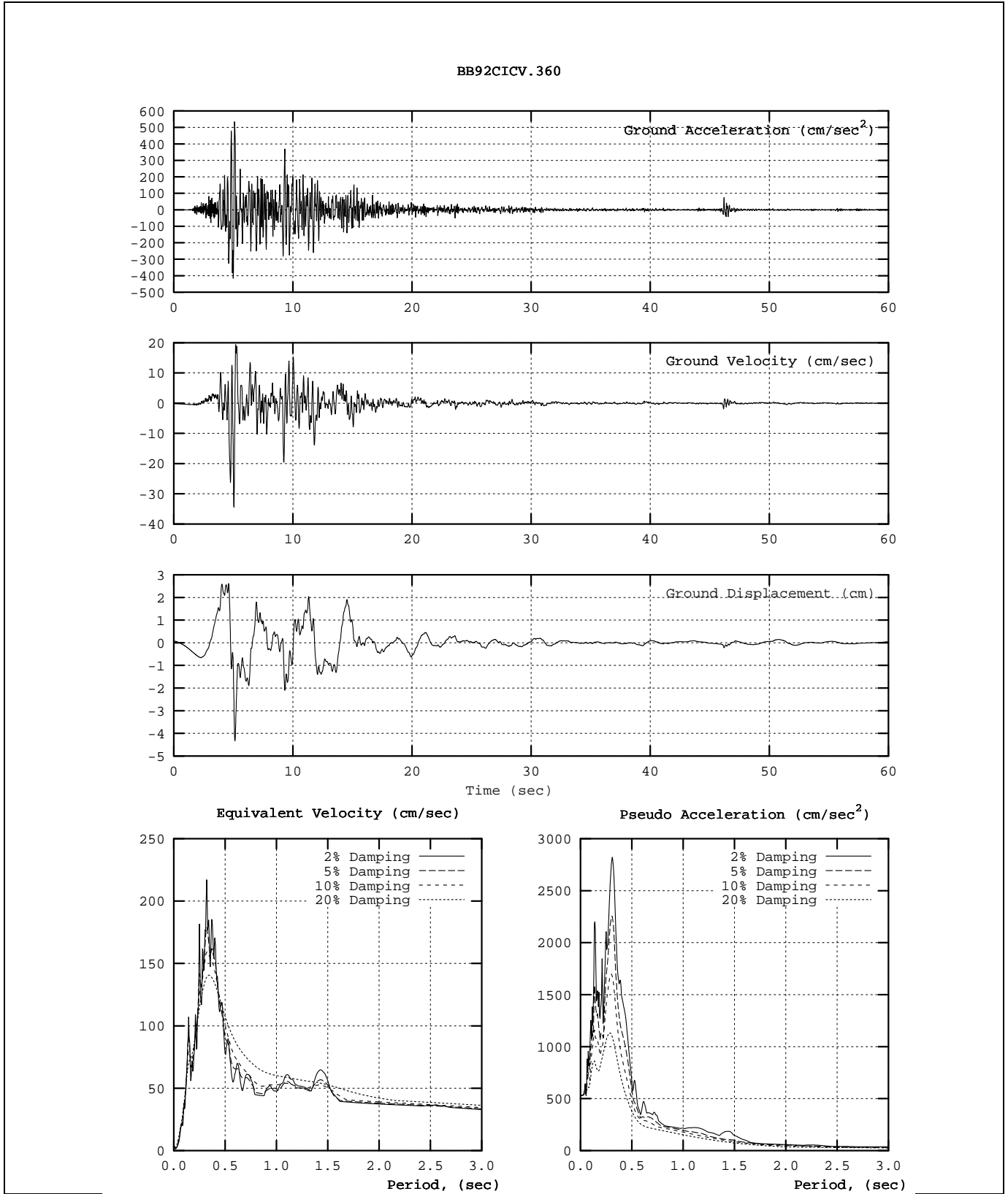


Figure 6-3 Characteristics of the BB92CIVC.360 (Big Bear) Ground Motion

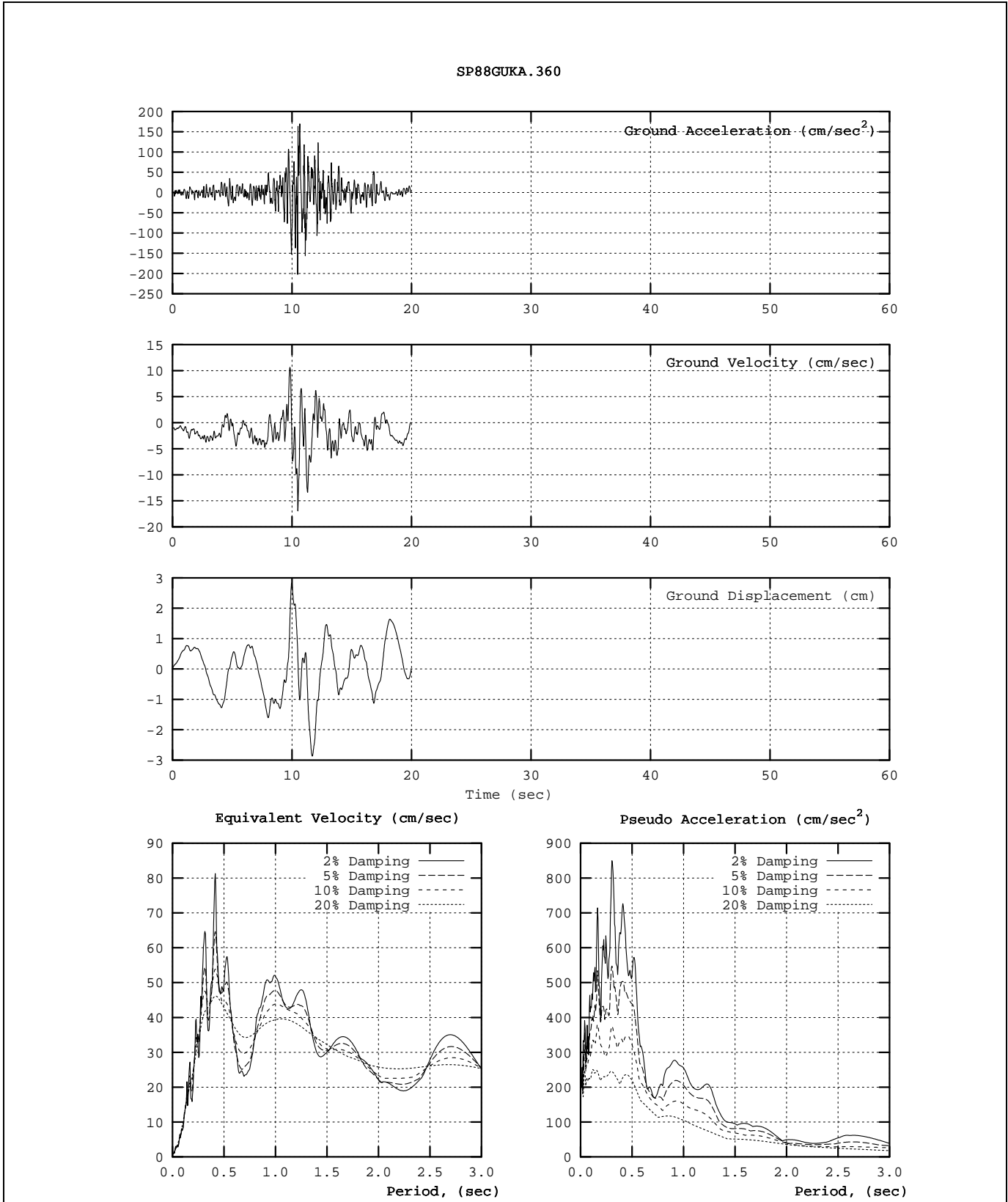


Figure 6-4 Characteristics of the SP88GUKA.360 (Spitak) Ground Motion

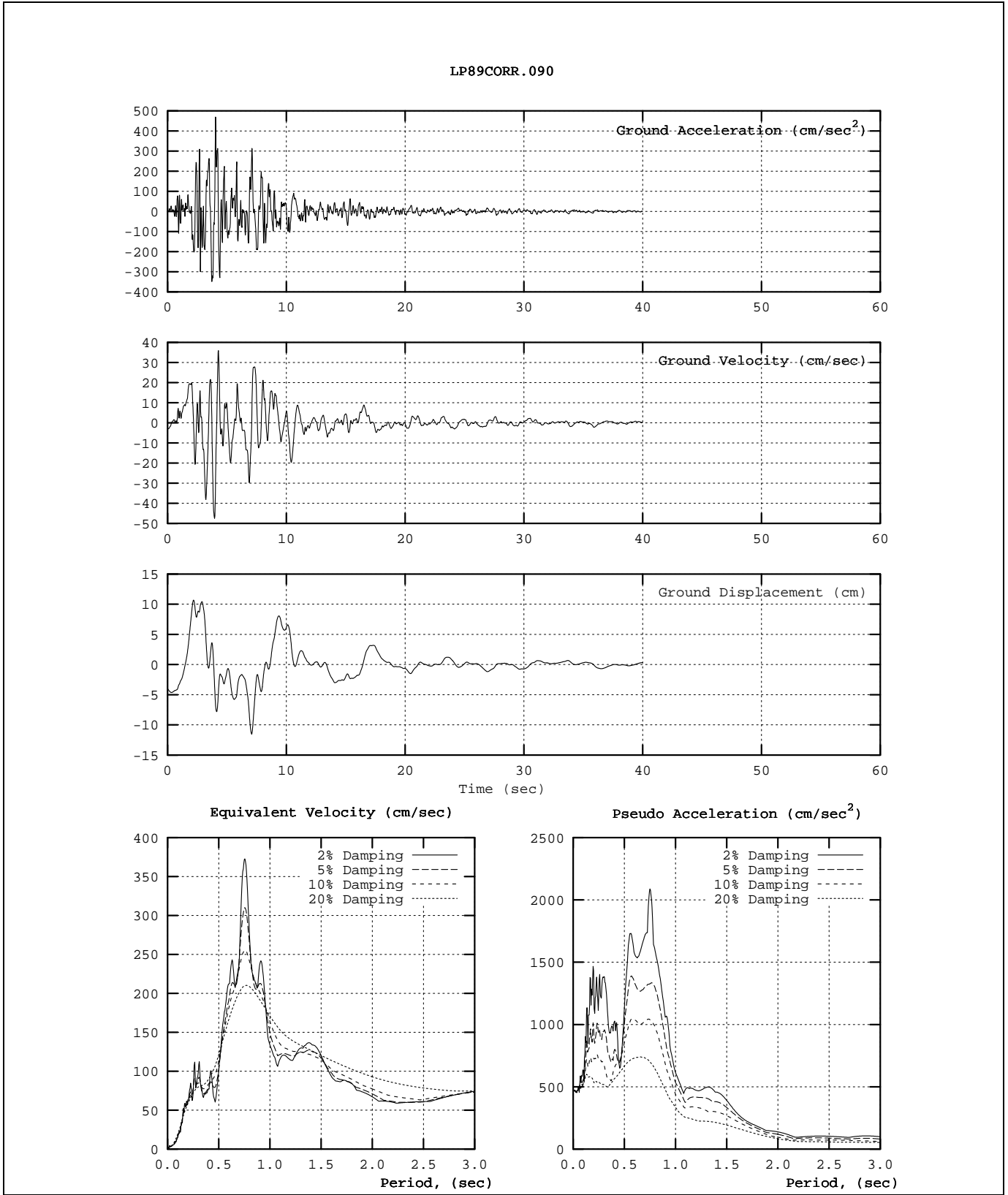


Figure 6-5 Characteristics of the LP89CORR.090 (Corralitos) Ground Motion

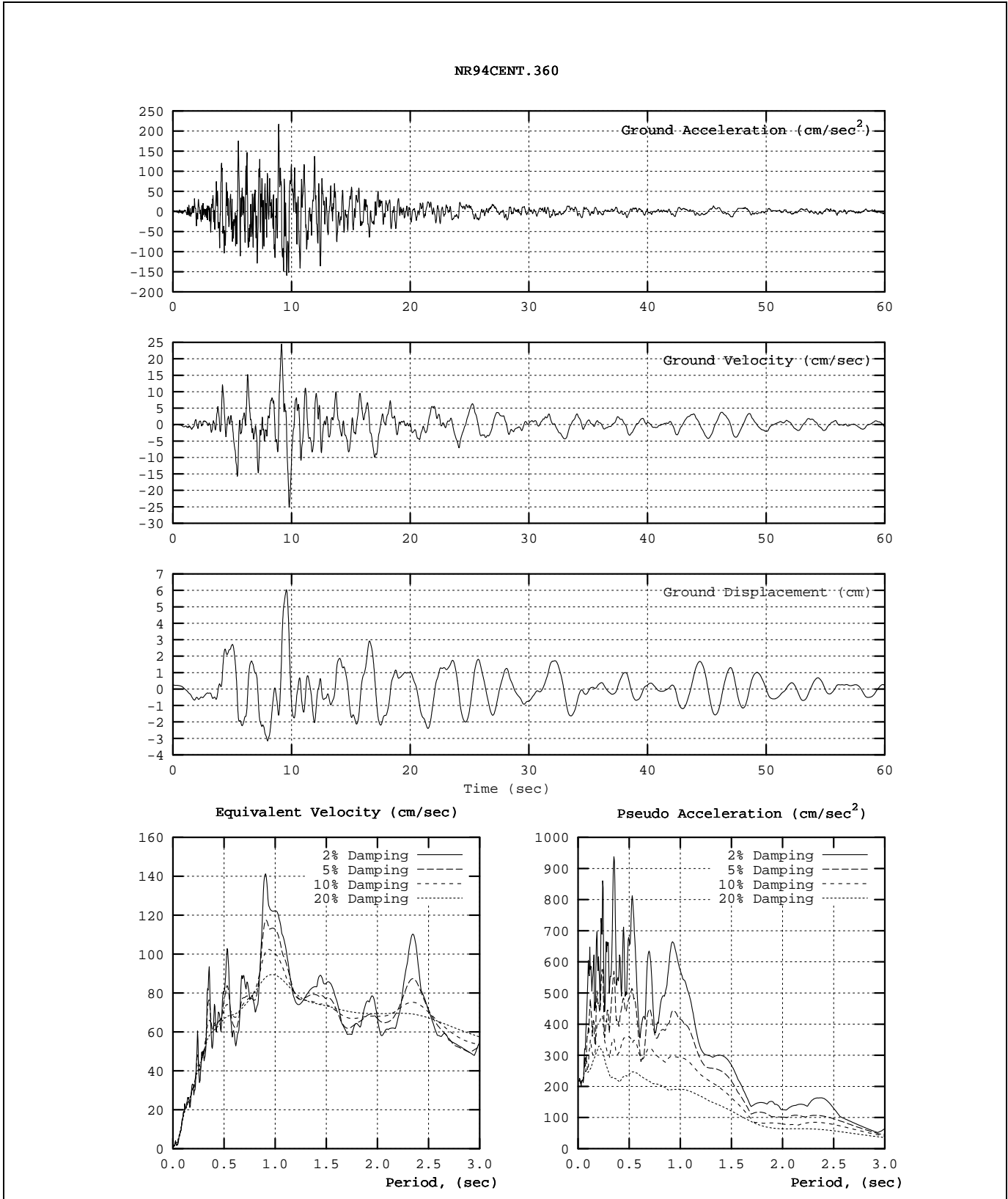


Figure 6-6 Characteristics of the NR94CENT.360 (Century City) Ground Motion

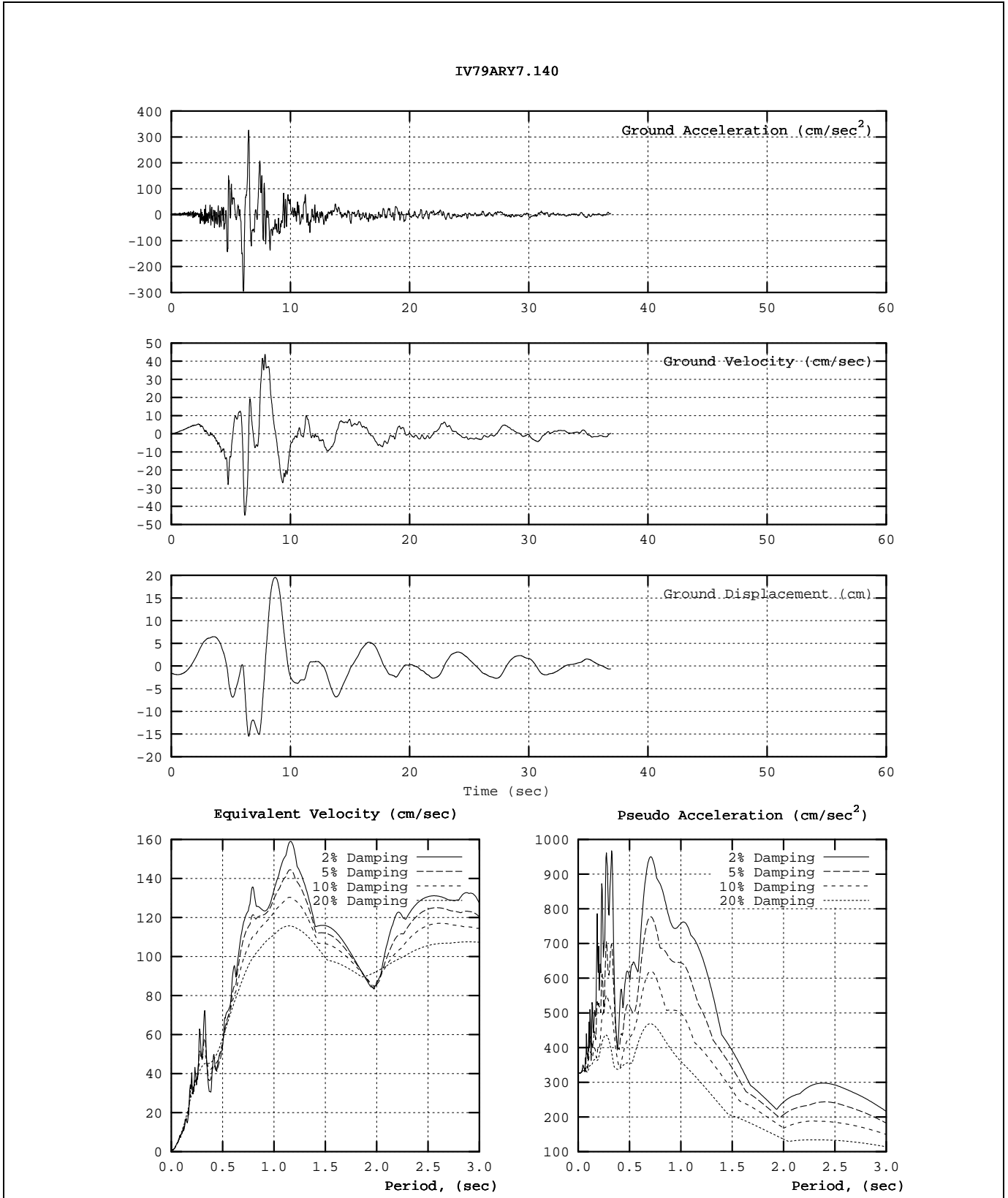


Figure 6-7 Characteristics of the IV79ARY7.140 (Imperial Valley Array) Ground Motion

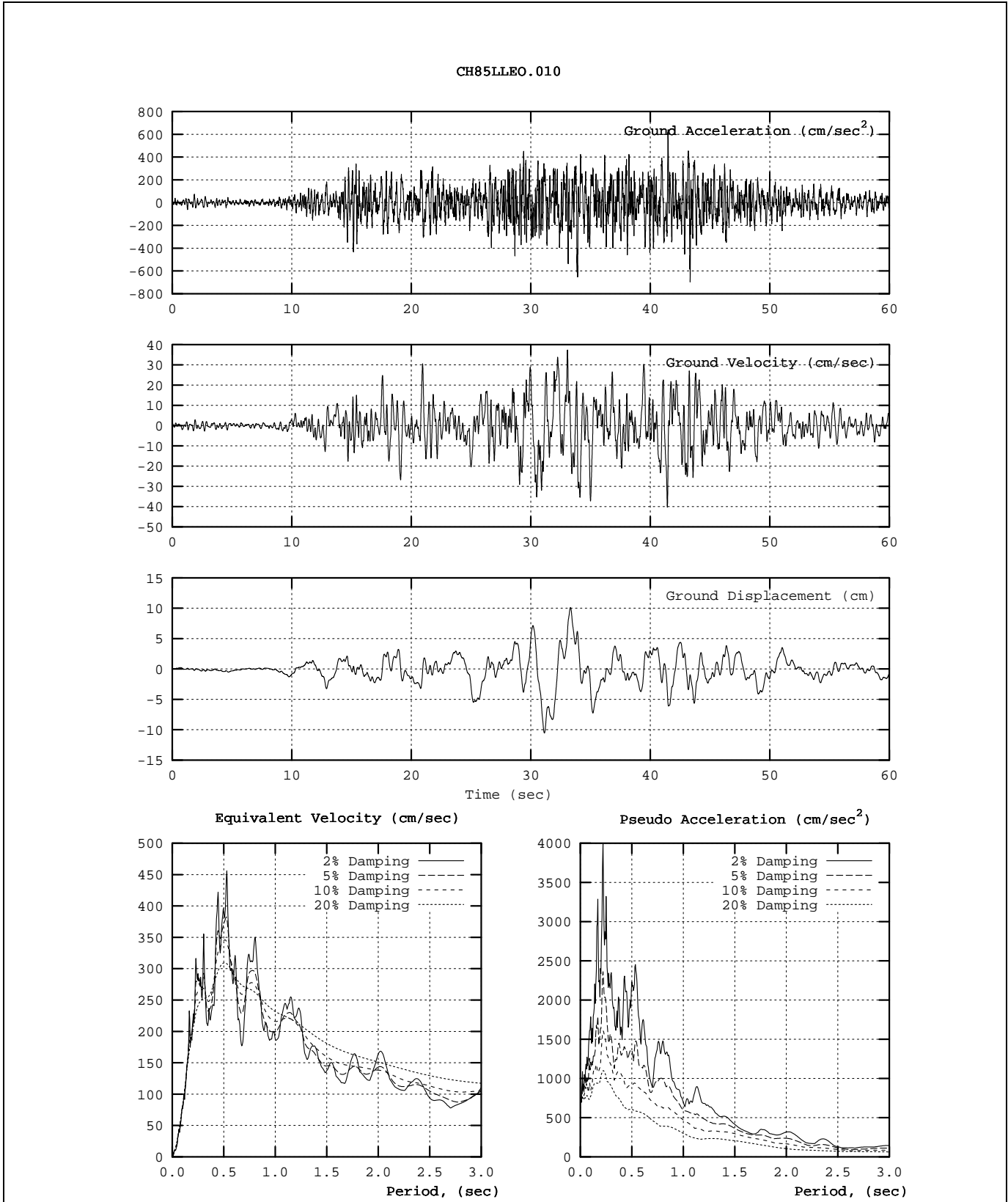


Figure 6-8 Characteristics of the CH85LLEO.010 (Llolleo) Ground Motion

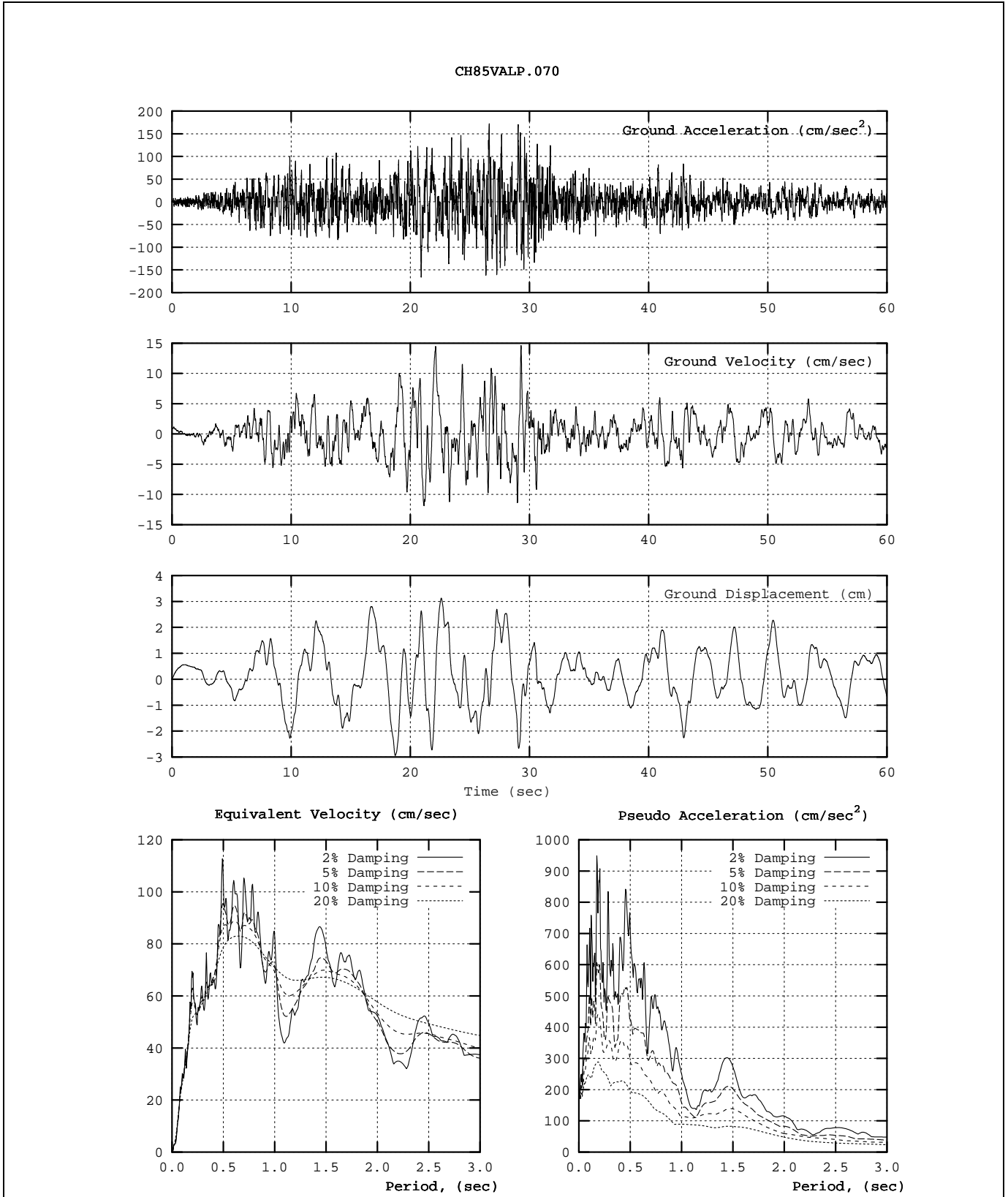


Figure 6-9 Characteristics of the CH85VALP.070 (Valparaiso University) Ground Motion

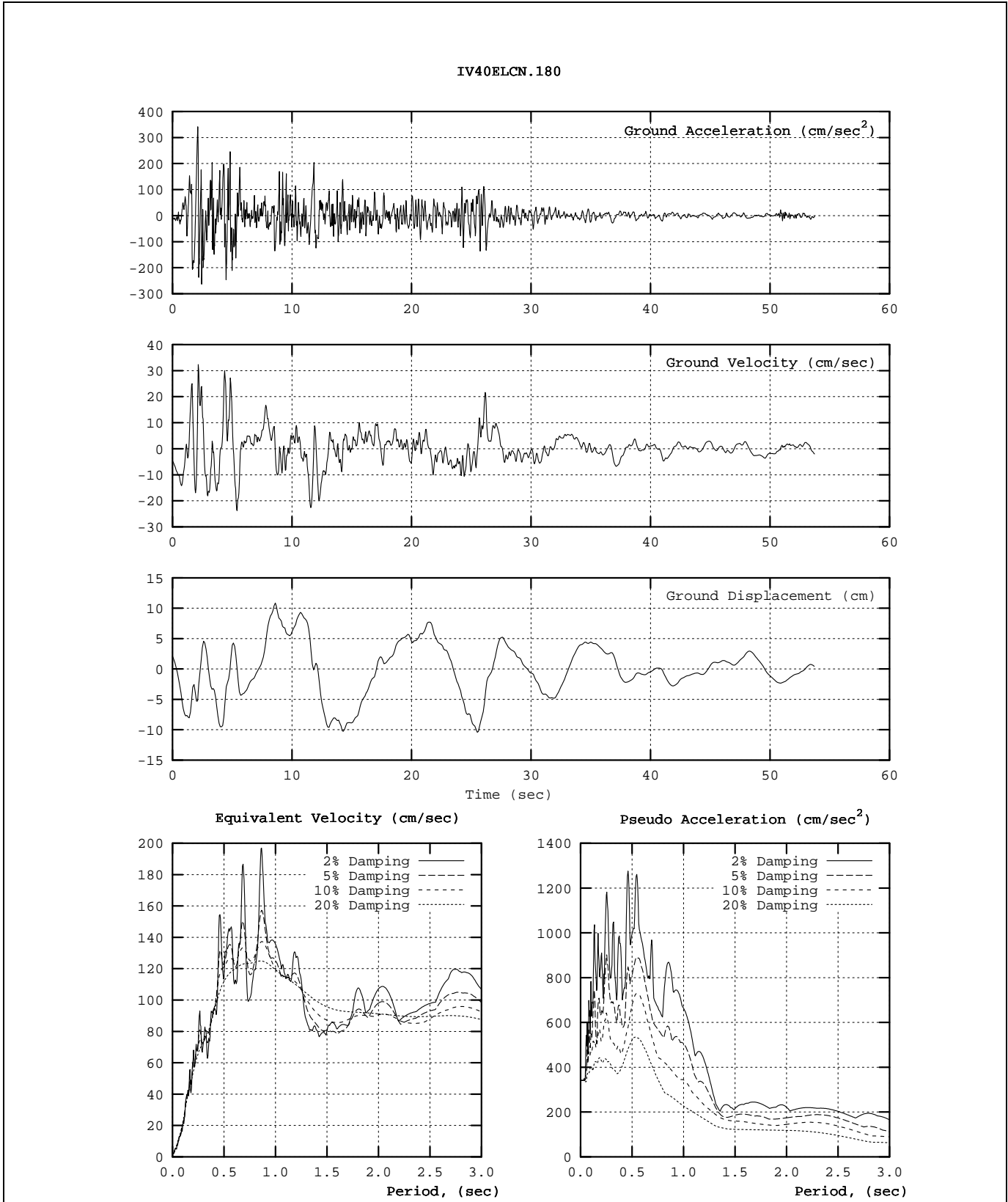


Figure 6-10 Characteristics of the IV40ELCN.180 (El Centro) Ground Motion

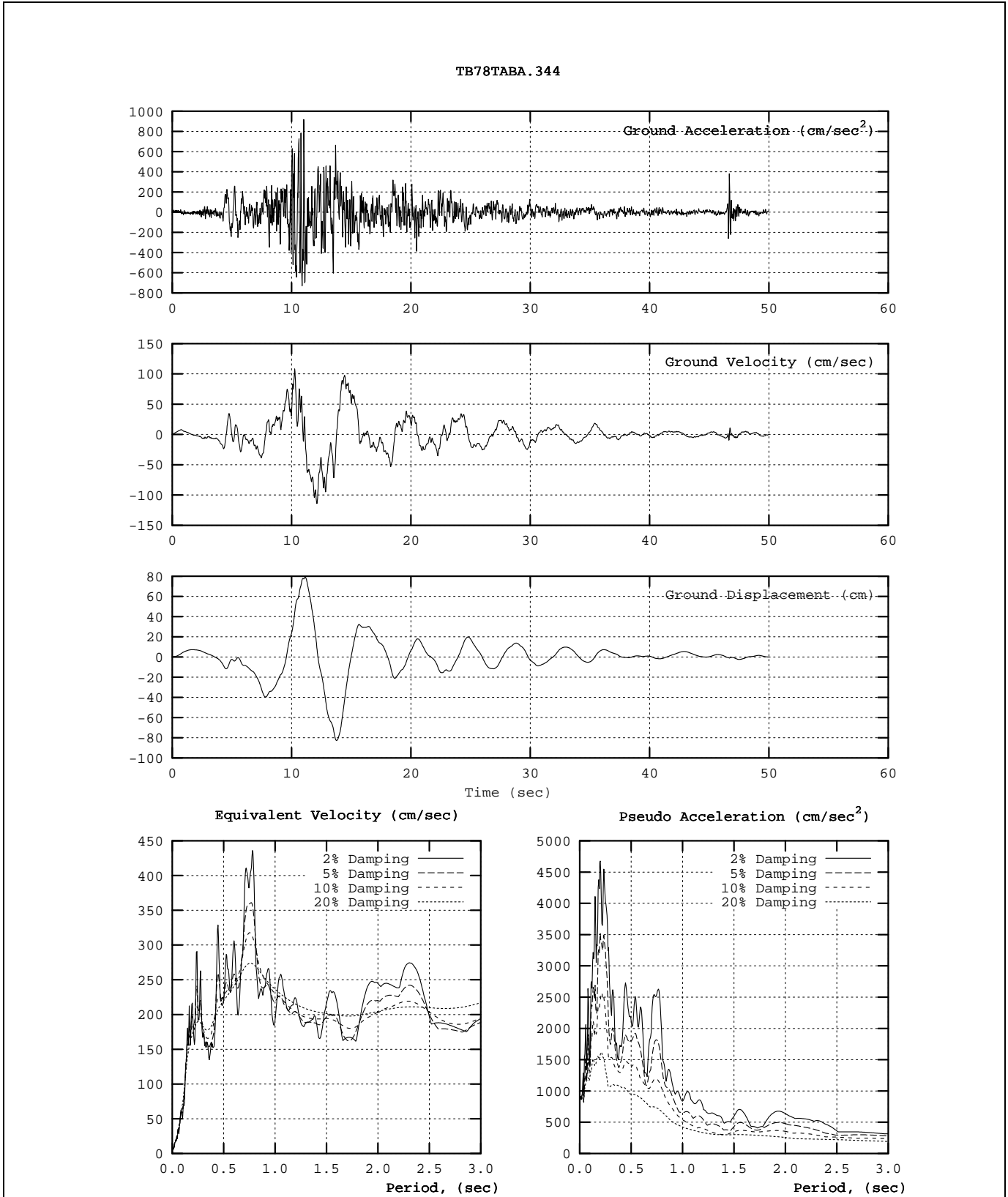


Figure 6-11 Characteristics of the TB78TABS.344 (Tabas) Ground Motion

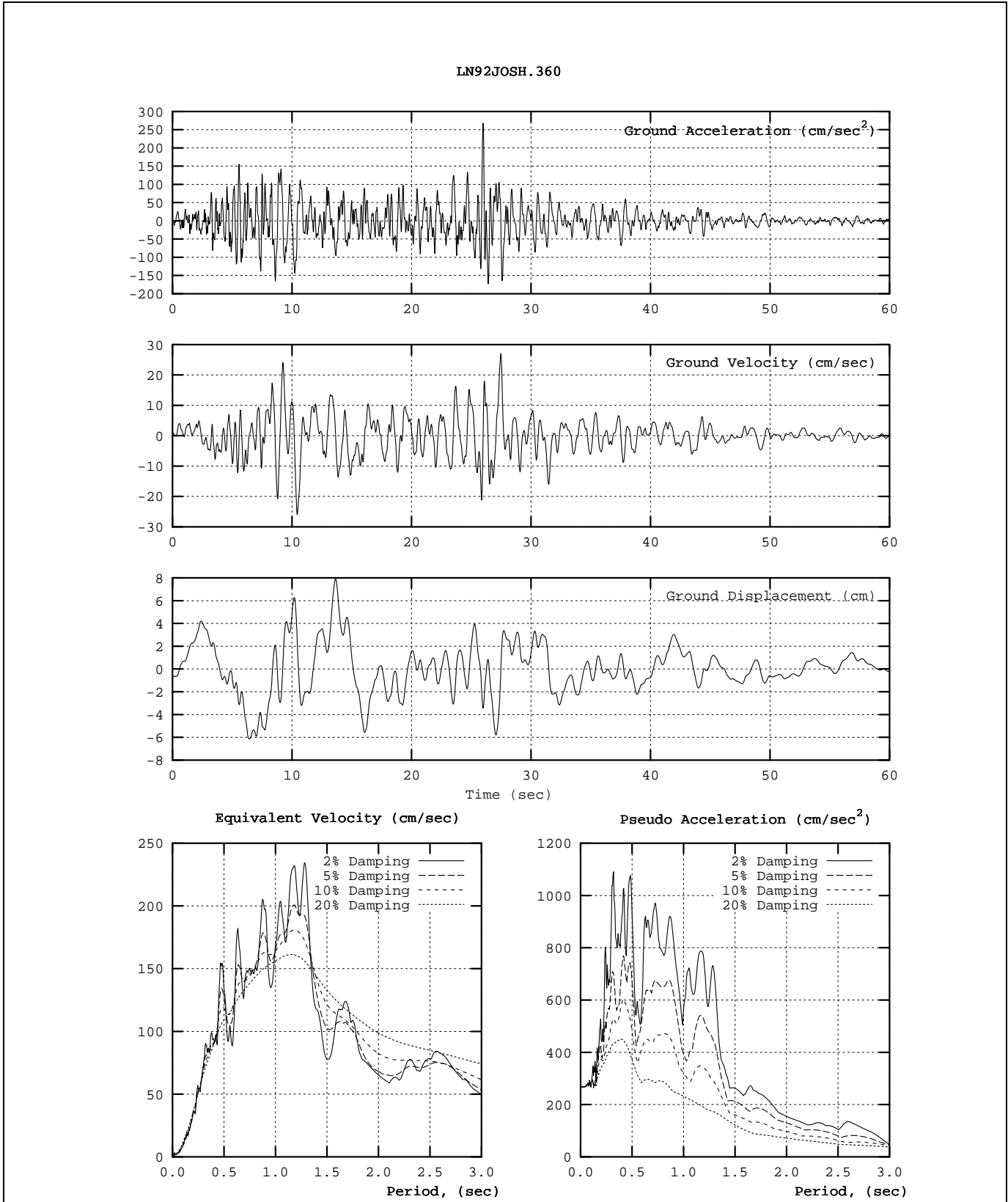


Figure 6-12 Characteristics of the LN92JOSH.360 (Joshua Tree) Ground Motion

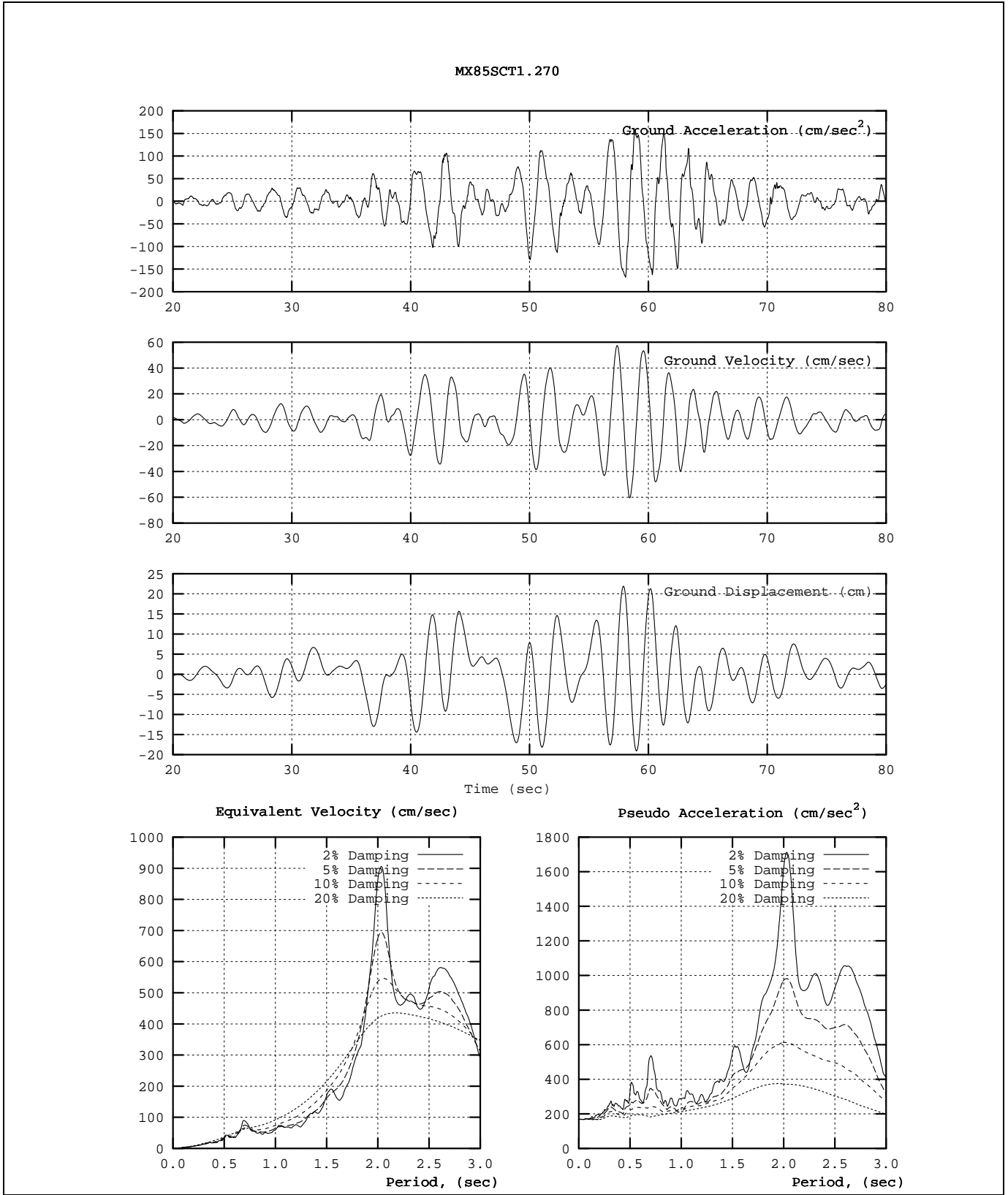


Figure 6-13 Characteristics of the MX85SCT1.270 (Mexico City) Ground Motion

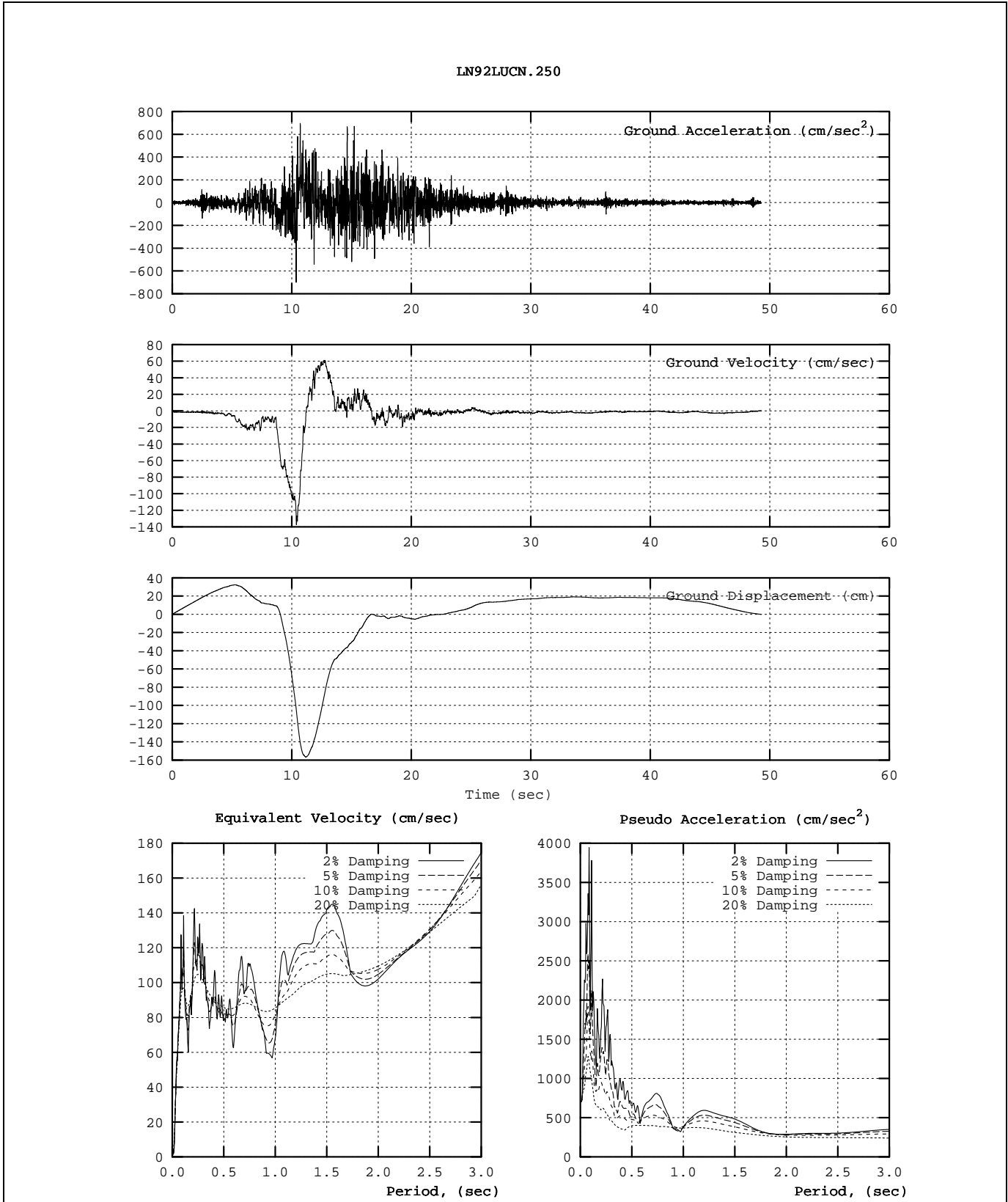


Figure 6-14 Characteristics of the LN92LUCN.250 (Lucerne) Ground Motion

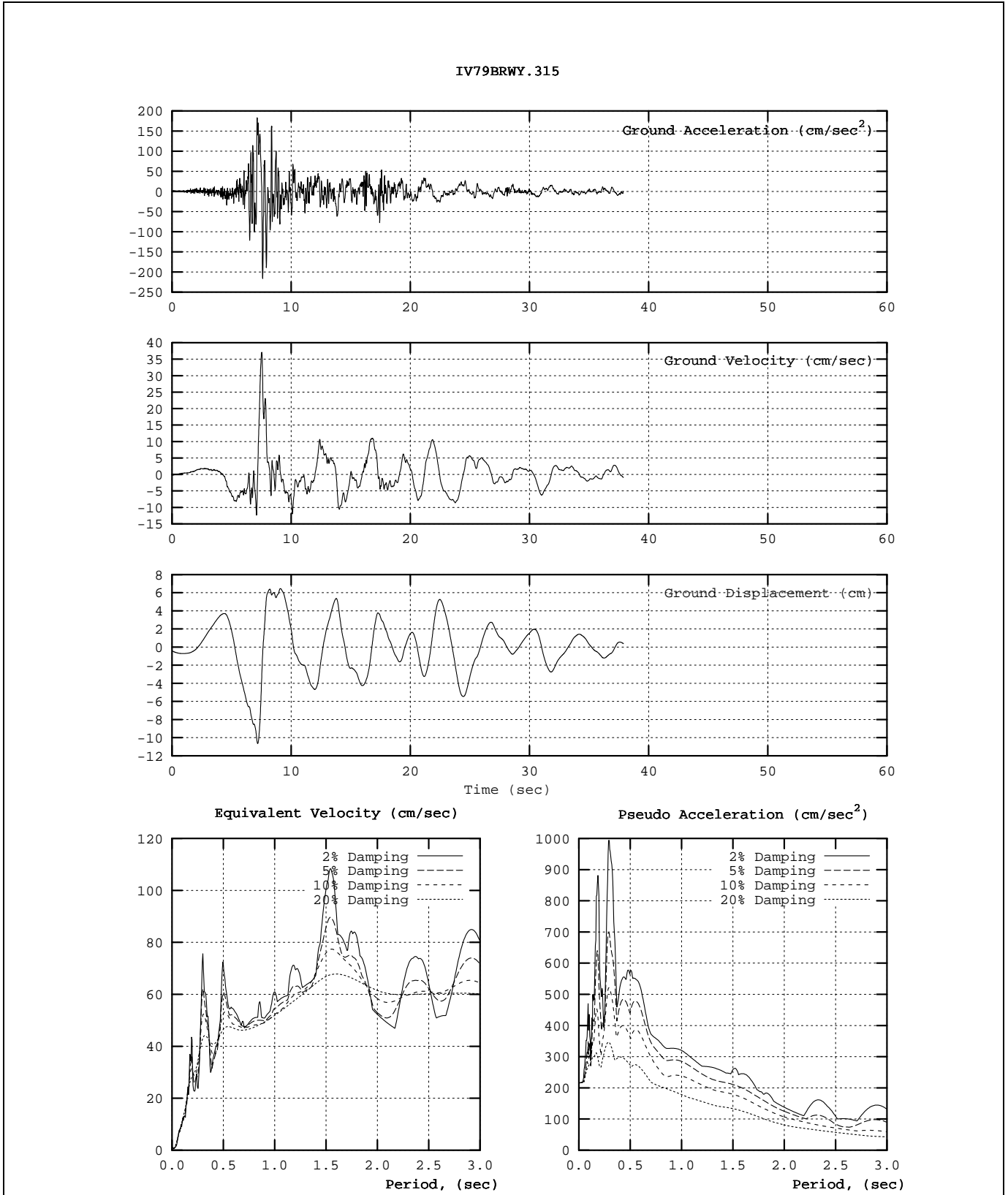


Figure 6-15 Characteristics of the IV79BRWY.315 (Brawley Airport) Ground Motion

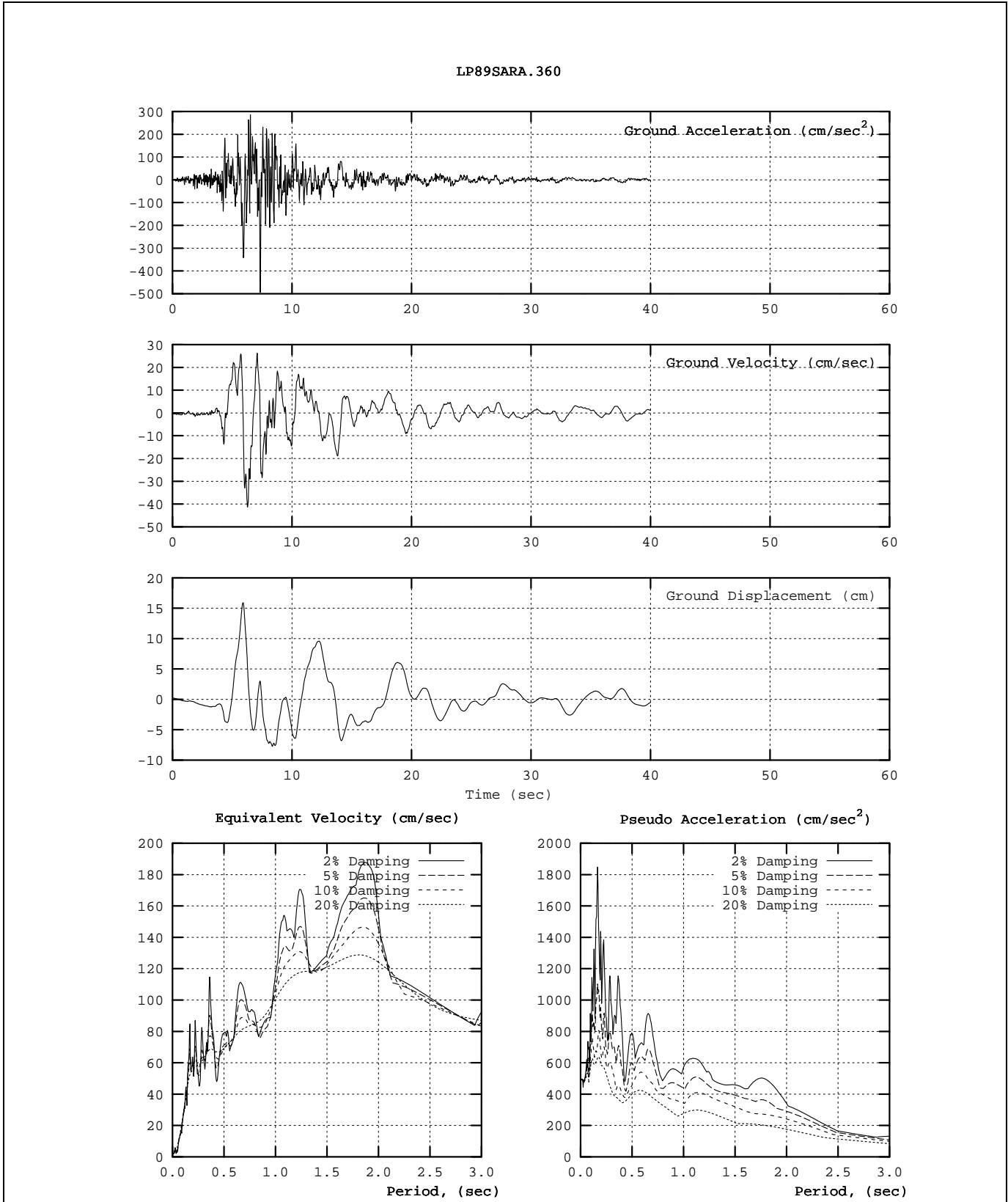


Figure 6-16 Characteristics of the LP89SARA.360 (Saratoga) Ground Motion

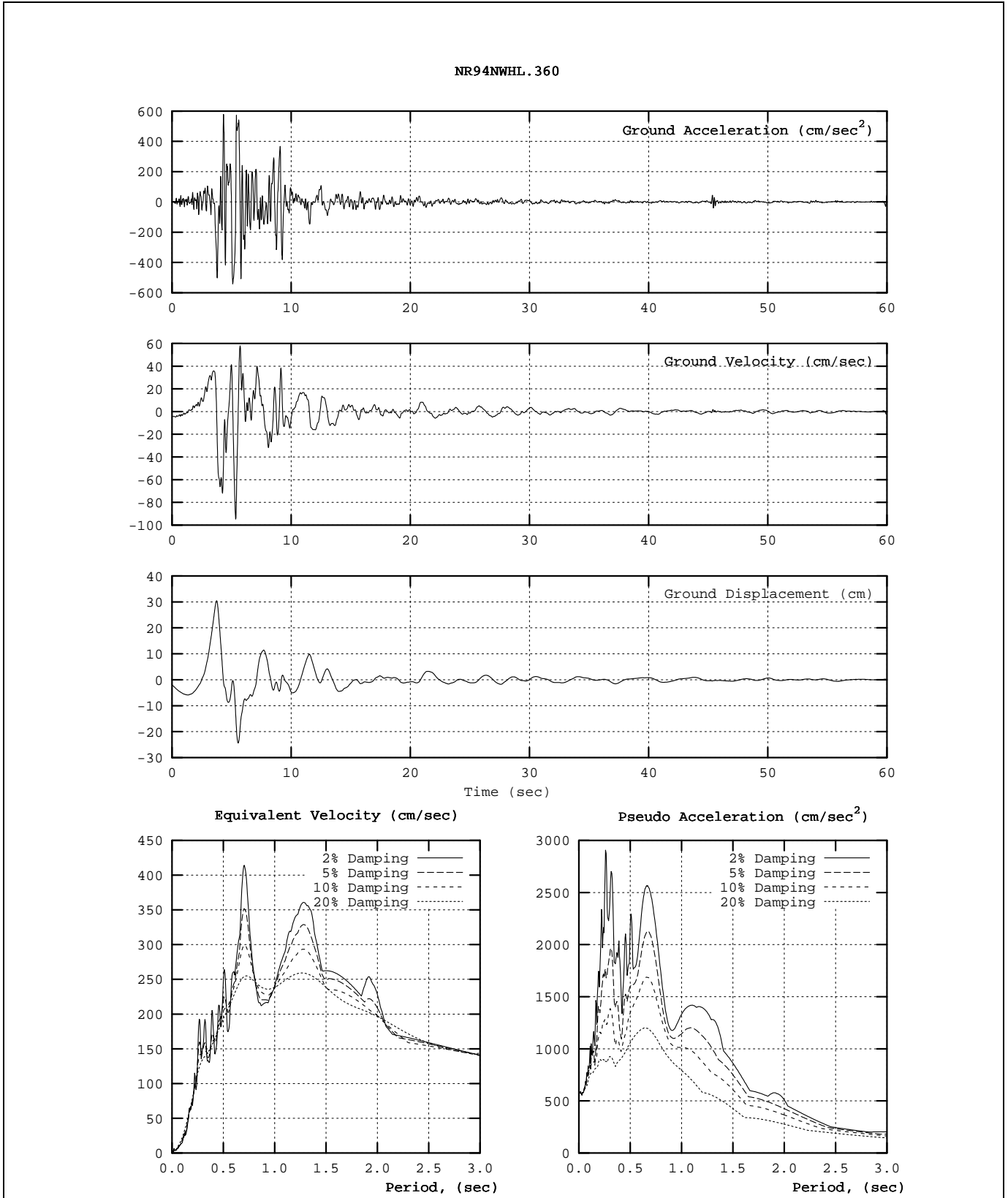


Figure 6-17 Characteristics of the NR94NWHL.360 (Newhall) Ground Motion

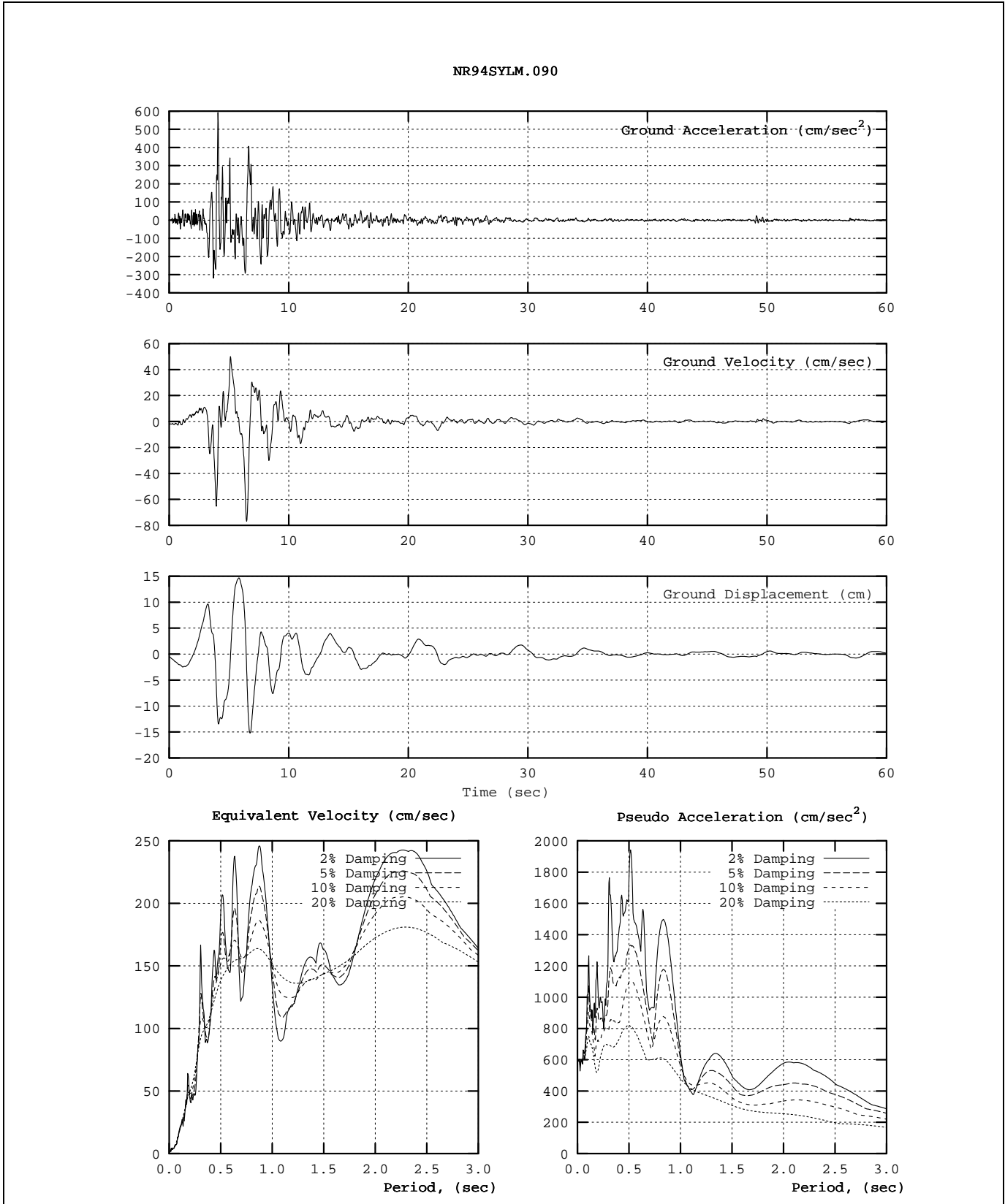


Figure 6-18 Characteristics of the NR94SYLM.090 (Sylmar Hospital) Ground Motion

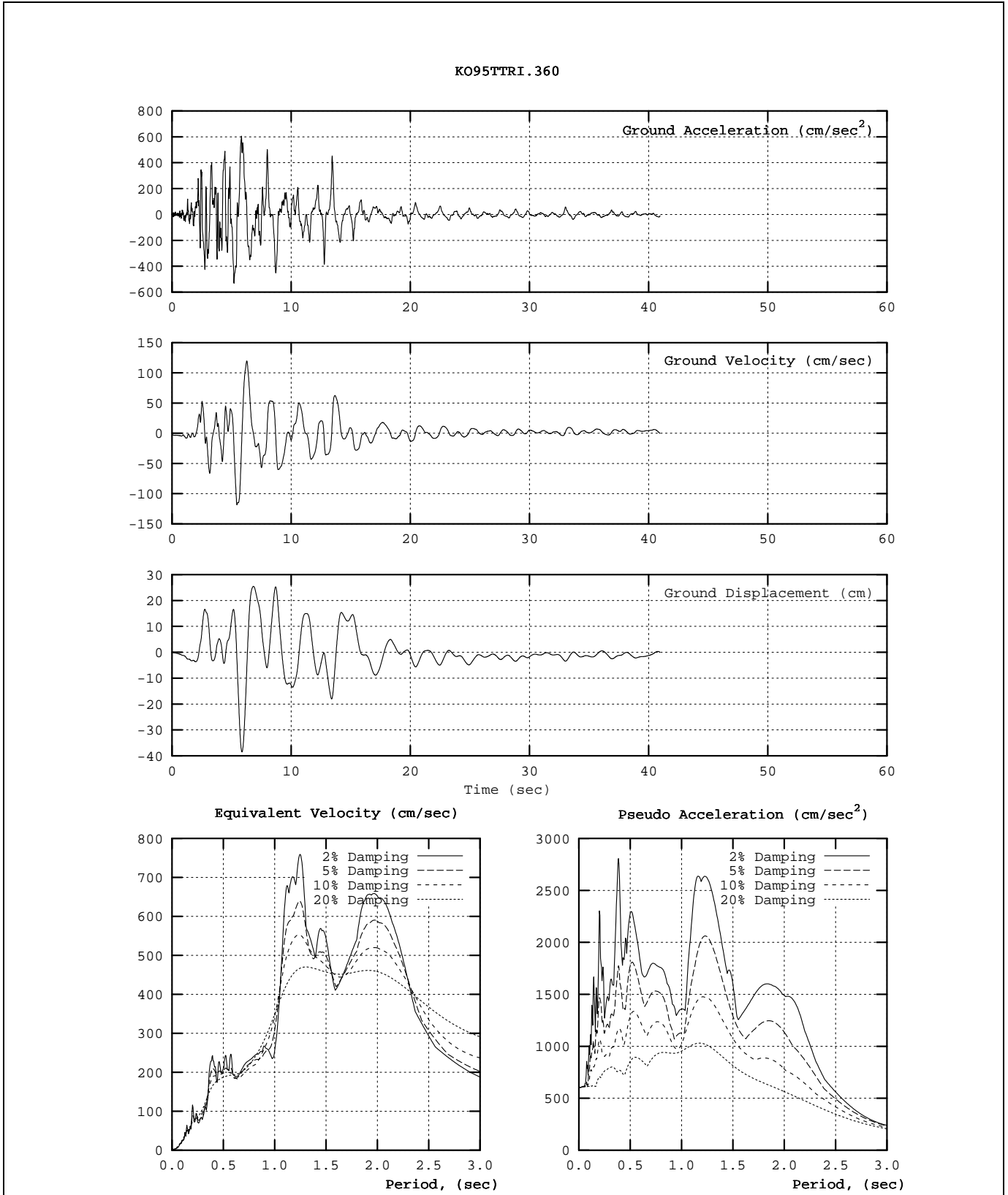


Figure 6-19 Characteristics of the KO95TTRI.360 (Takatori) Ground Motion

The characteristic period,  $T_g$ , of each ground motion was established assuming equivalent-velocity spectra and pseudo-acceleration spectra for linear elastic oscillators having 5% damping. The equivalent velocity,  $V_m$ , is related to input energy,  $E_m$ , and ground acceleration and response parameters by the following expression:

$$\frac{1}{2} m V_m^2 = E_m = m \int \ddot{x}_g \dot{x} dt \quad (6-1)$$

where  $m$  = mass of the single-degree-of-freedom oscillator,  $\ddot{x}_g$  = the ground acceleration, and  $\dot{x}$  = the relative velocity of the oscillator mass (Shimazaki and Sozen, 1984). The spectra present peak values calculated over the duration of the record.

The characteristic periods were determined according to engineering judgment to correspond approximately to the first (lowest-period) peak of the equivalent-velocity spectrum, and, at the same time, the period at which the transition occurs between the constant-acceleration and constant-velocity portions of a smooth design spectrum fitted to the 5% damped spectrum (Shimazaki and Sozen, 1984; Qi and Moehle, 1991; and Lepage, 1997). Characteristic periods were established prior to the dynamic analyses.

Other criteria are available to establish characteristic periods. For example, properties of the site, characterized by variation of shear-wave velocity with depth, may be used to establish  $T_g$ . Alternatively, the characteristic period may be defined as the lowest period for which the equal-displacement rule applies,

and thus becomes a convenient reference point to differentiate between short- and long-period systems.

### 6.3.4 Force/Displacement Models

The choice of force/displacement model influences the response time-history and associated peak response quantities. Ideally, the force/displacement model should represent behavior typical of wall buildings, including strength degradation and stiffness degradation.

Actual response depends on the details of structural configuration and component response, which in turn, depend on the material properties, dimensions, and strength of the components, as well as the load environment and the evolving dynamic load history (which can influence the type and onset of failure). The objective of the dynamic analyses is to identify basic trends in how prior damage affects system response in future earthquakes. Fulfilling this objective does not require the level of modeling precision that would be needed to understand the detailed response of a particular structure or component. For this reason, we selected relatively simple models that represent a range of behaviors that might be expected in wall buildings. Three broad types of system response can be distinguished:

- Type A: Stiffness-degrading systems with positive post-yield stiffness (Figure 6-20a).
- Type B: Stiffness-degrading systems with negative post-yield stiffness (Figure 6-20b).
- Type C: Pinched systems exhibiting strength and stiffness degradation (Figure 6-20c).

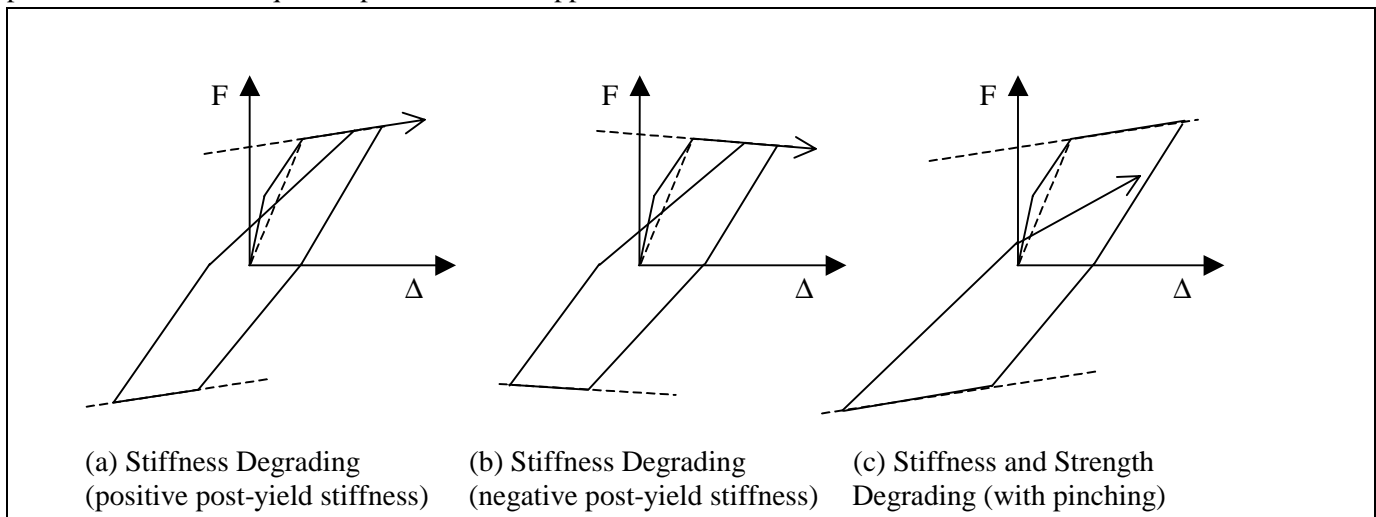


Figure 6-20 Force-Displacement Hysteretic Models

Type A behavior typically represents wall systems dominated by flexural response. Type B behavior is more typical of wall systems that exhibit some degradation in response with increasing displacement; degradation may be due to relatively brittle response modes. Type C behavior is more typical of wall systems that suffer degradation of strength and stiffness, including those walls in which brittle modes of response may predominate.

Type A behavior was represented in the analyses using the Takeda model (Takeda et al., 1970) with post-yield stiffness selected to be 5% of the secant stiffness at the yield point (Figure 6-21a). Previous experience (Section 6.2.1) indicates that this model represents stiffness degradation in reinforced concrete members exceptionally well. In addition, it is widely known by researchers, and it uses displacement ductility to parameterize stiffness degradation. The Takeda model features a trilinear primary curve that is composed of uncracked, cracked, and yielding portions. After yielding, the unloading stiffness is reduced in proportion to the square root of the peak displacement ductility. Additional rules are used to control other aspects of this hysteretic model. This model is subsequently referred to as “Takeda5”.

Type B behavior was represented in the analyses using the Takeda model with post-yield stiffness selected to be -10% of the yield-point secant stiffness (Figure 6-21b). This model is subsequently referred to as “Takeda10”.

Type C behavior was represented in the analyses by a modified version of the Takeda model (Figure 6-21c). The behavior is the same as for Type A, except for modifications to account for pinching and cyclic strength degradation. The pinching point is defined independently in the first and third quadrants (Figure 6-22). The pinching-point displacement is set equal to 30% of the current maximum displacement in the quadrant. The pinching-point force level is set equal to 10% of the current maximum force level in the quadrant. Cyclic strength degradation incorporated in this model is described in Section 6.3.6. This model is subsequently referred to as “TakPinch”.

Collectively, the Takeda5, Takeda10, and TakPinch models are referred to as degrading models in the body of this section. For these models, dynamic analyses were used to identify the effects of prior damage on response to future earthquakes. The analyses covered a number of relative strength values, initial periods of vibration, damage intensities, and performance-level earthquakes. For all dynamic analyses, damping was set equal to 5% of critical damping, based on the period of vibration that corresponds to the yield-point secant stiffness.

In addition, a bilinear model (Figure 6-23) was selected to establish the strength of the degrading oscillators, which were set equal to the strength required to achieve bilinear displacement ductility demands of 1 (elastic), 2, 4, and 8 for each reference period and for each of the 18 ground motions. The bilinear model does not exhibit stiffness or strength degradation. Besides establishing

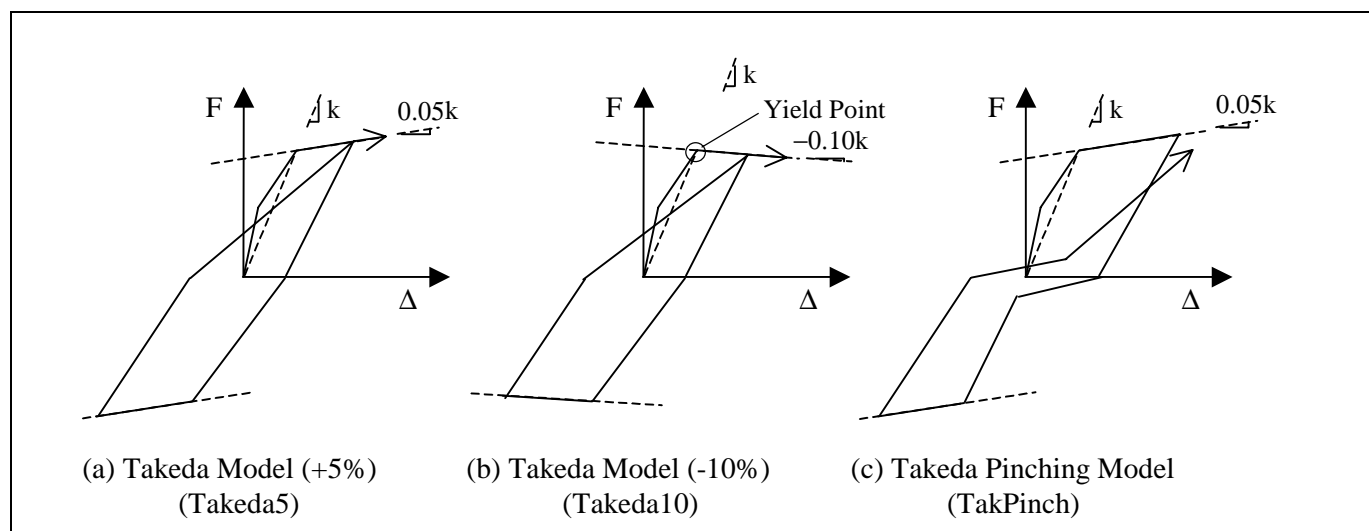


Figure 6-21 Degrading Models Used in the Analyses

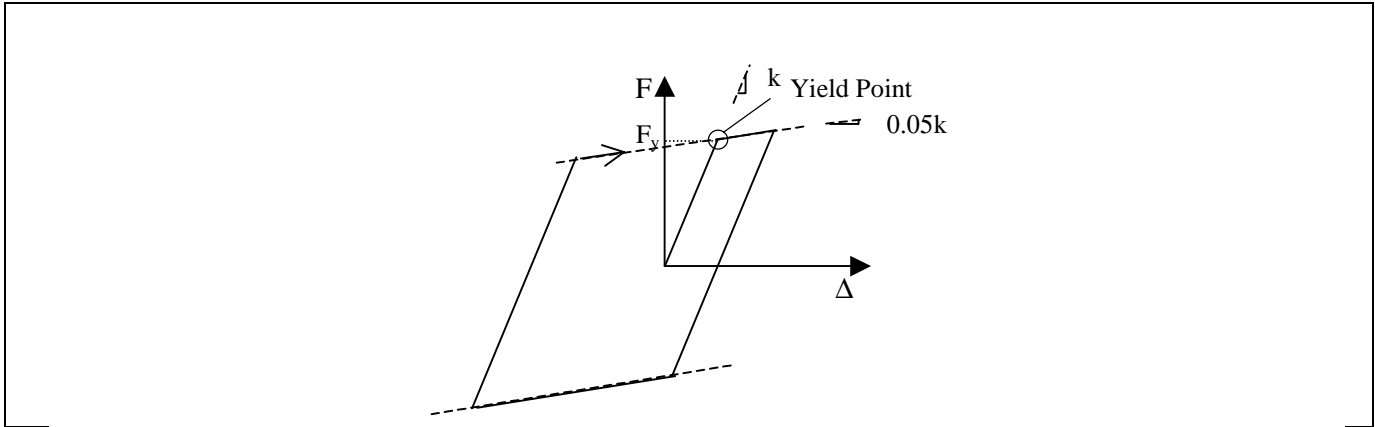


Figure 6-22 Bilinear Model Used to Determine Strengths of Degrading Models

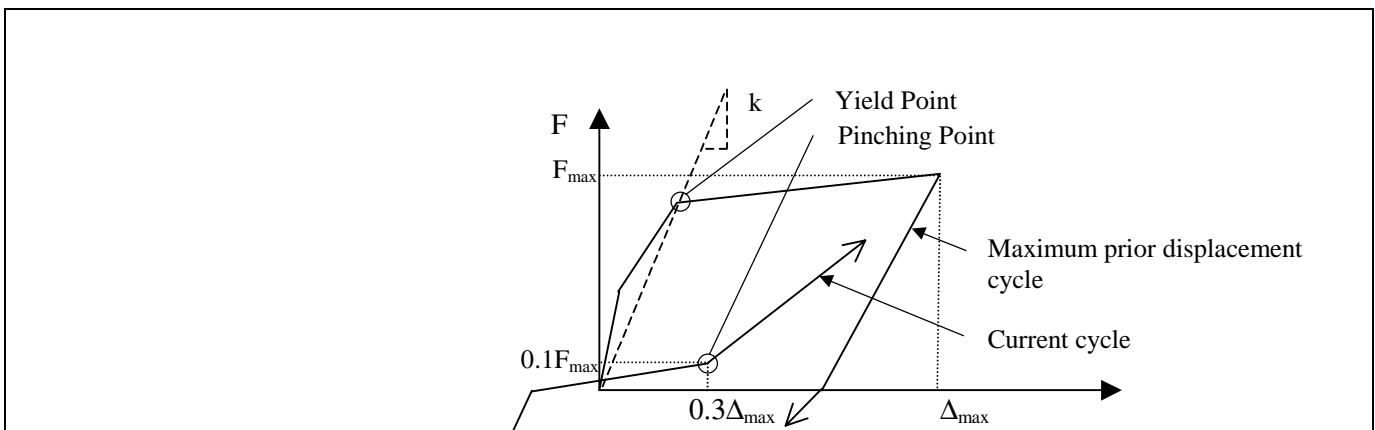


Figure 6-23 Specification of the Pinching Point for the Takeda Pinching Model

the strength of the oscillators, this model serves two additional purposes. First, results obtained in this study with the bilinear model can be compared with those obtained by other researchers to affirm previous findings and, at the same time, to develop confidence in the methods and techniques used in this study. Second, the bilinear model provides a convenient point of departure from which the effects of stiffness and strength degradation can be compared.

### 6.3.5 Undamaged Oscillator Parameters

To identify effects of damage on response, it is first necessary to establish the response of initially-undamaged oscillators to the same ground motions. The response of the undamaged oscillators is determined using the degrading models of Figure 6-21 for the performance-level ground motions.

The yield strength of all degrading models is set equal to the strength required to achieve displacement

ductility demands (DDD) of 1 (elastic), 2, 4, and 8 using the bilinear model. This is done at each period and for each ground motion. For any period and ground motion considered, the yield strength of the initially-undamaged models is the same, but only the bilinear model achieves the target displacement ductility demand. Where the same target displacement ductility demand can be achieved for various strength values, the largest strength value is used, as implemented in the computer program PCNSPEC (Boroschek, 1991).

The initial stiffness of the models is established to achieve initial (reference) vibration periods of 0.1, 0.2, 0.3, 0.4, 0.5, 0.6, 0.8, 1.0, 1.2, 1.5, and 2.0 seconds. These periods are determined using the yield-point secant stiffness for all the models considered.

For the undamaged Takeda models, the cracking strength is set equal to 50% of the yield strength, and the uncracked stiffness is set equal to twice the yield-point secant stiffness (Figure 6-24).

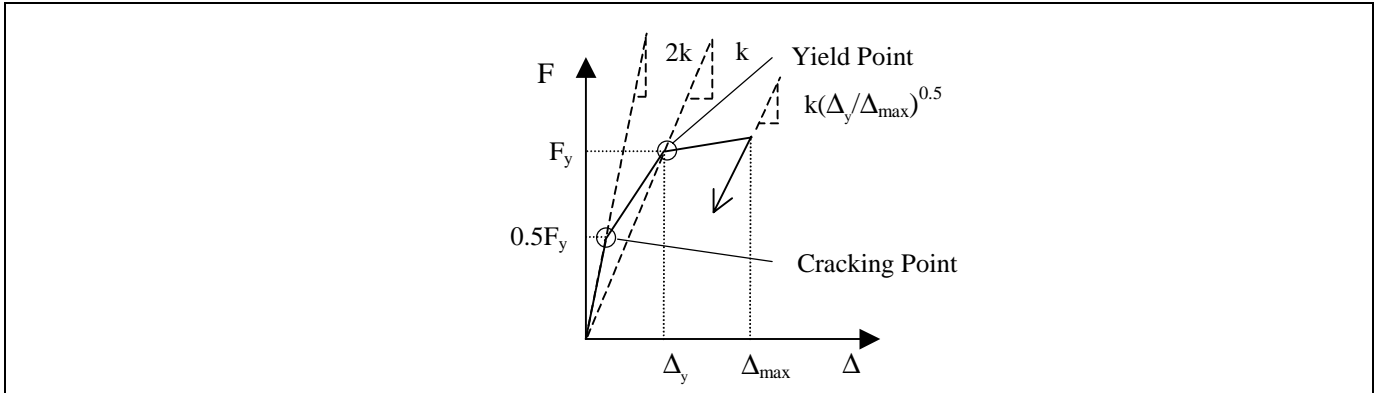


Figure 6-24 Specification of the Uncracked Stiffness, Cracking Strength, and Unloading Stiffness for the Takeda Models

### 6.3.6 Damaged Oscillator Parameters

Damage is considered by assuming that the force-displacement curves of the oscillators are altered as a result of previous inelastic response. Reduction in stiffness caused by the damaging earthquake is parameterized by prior ductility demand. Strength degradation is parameterized by the reduced strength ratio.

Each of the initially-undamaged degrading oscillators is considered to have experienced prior ductility demand (PDD) equal to 1, 2, 4, or 8 as a result of the damaging earthquake. The construction of an initially-damaged oscillator force/displacement curve is illustrated for a value of PDD greater than zero in Figure 6-25. The prior ductility demand also regulates the unloading stiffness of the Takeda model until larger displacement ductility demands develop.

The analytical study considered damaging earthquakes of smaller intensity than the performance-level earthquake. Consequently, the PDD values considered must be less than or equal to the design displacement ductility (DDD). Thus, an oscillator with strength established to achieve a displacement ductility of 4 is analyzed only for prior displacement ductility demands of 1, 2, and 4. The undamaged Takeda oscillators sometimes had ductility demands for the performance-level earthquake that were lower than their design values (DDD). Again, because the damaging earthquake is considered to be less intense than the performance-level event, oscillators having PDD in excess of the undamaged oscillator response were not considered further.

The Takeda models of the undamaged oscillators represent cracking behavior by considering the uncracked stiffness and the cracking strength. The effects of cracking in a previous earthquake were assessed by comparing the peak displacement response

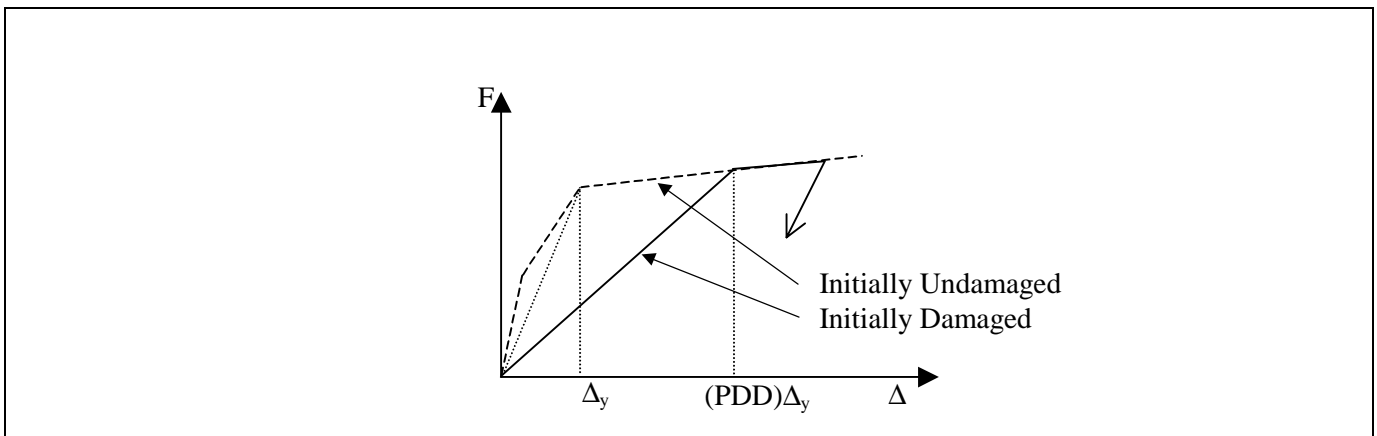
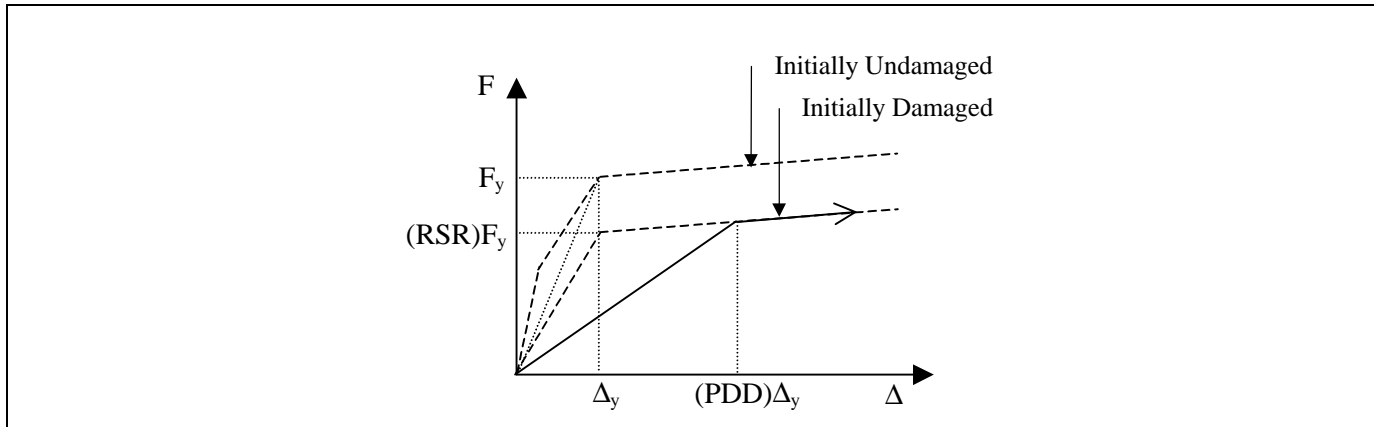


Figure 6-25 Construction of Initial Force-Displacement Response for Prior Ductility Demand > 0 and Reduced Strength Ratio = 1



**Figure 6-26** Construction of Initial Force-Displacement Response for  $PDD > 0$  and  $RSR < 1$  for Takeda5 and Takeda10 Models

of initially-uncracked oscillators to the response of oscillators that are initially cracked; that is, Takeda oscillators having a PDD of one. When larger PDD values are considered, the reductions in initial loading and unloading stiffness are determined in accordance with the Takeda model.

It is not obvious what degree of strength degradation is consistent with the PDDs, nor just how the degradation of strength should be modeled to represent real structures. We used two approaches to gauge the extent to which strength degradation might affect the response:

1. **Takeda5 and Takeda10 Oscillators:** The initial strength of the damaged models was reduced to try to capture the gross effects of strength degradation on response. The initial response of the damaged oscillator was determined using the construction of Figure 6-26. The resulting curve may represent a backbone curve that is constructed to approximate the response of a strength-degrading oscillator. For example, a structure for which repeated cycling causes a 20% degradation in strength relative to the primary curve may be modeled as having an initial strength equal to 80% of the undegraded strength.

If the backbone curve is established using the expected degraded-strength asymptotes, then the modeled structure tends to have smaller initial stiffness and larger displacement response relative to the ideal degrading structure. Consequently, the modeled response is expected to give an upper bound to the displacement response expected from the ideal model. If, instead, the backbone curve is selected to represent an average degraded response, using typical degraded-strength values rather than the lower asymptotic values, the computed response

should more closely approximate the response of the ideal model.

2. **TakPinch Oscillators:** Rather than begin with a reduced strength, a form of cyclic strength degradation was explicitly modeled for the Takeda Pinching oscillators. A trilinear primary curve was established (Figure 6-27), identical to the envelope curve used in the Takeda5 model. The curve exhibits cracking, a yield strength determined from the response of the bilinear models, and a post-yield stiffness equal to 5% of the yield-point secant stiffness. A secondary curve is established, having the same yield displacement and post-yield stiffness as the primary curve, but having yield strength equal to the reduced strength ratio (RSR) times the primary yield strength. For displacements less than the current maximum displacement in the quadrant, a reduced-strength point is defined at the maximum displacement at  $0.5^n(1-RSR)F_y$ , above the secondary curve strength, where  $n$  is the number of cycles approaching the current maximum displacement. The oscillator may continue beyond this displacement, and once it loads along the primary curve,  $n$  is reset to one, to cause the next cycle to exhibit strength degradation. The term  $(1-RSR)F_y$  is simply the strength difference between the primary and secondary curves, and the function  $0.5^n$  represents an asymptotic approach toward the secondary curve with each cycle. In each cycle, the strength is reduced by half the distance remaining between the current curve and the secondary curve. Pinching and strength degradation are modeled independently in the first and third quadrants.

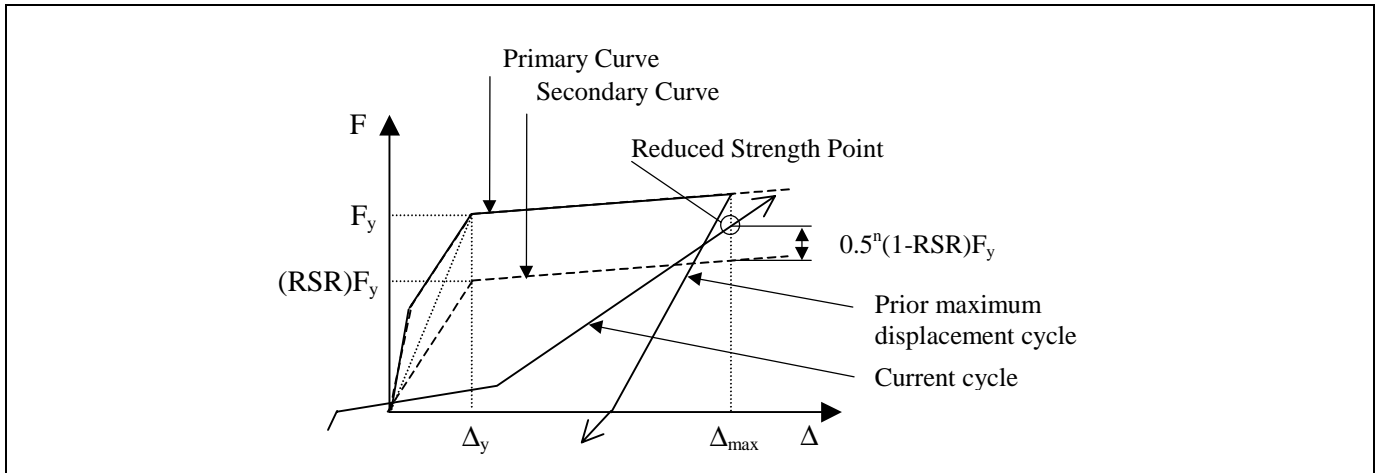


Figure 6-27 Strength Degradation for Takeda Pinching Model

For the TakPinch models, strength degradation is modeled with and without PDD. When PDD is present, the oscillator begins with  $n$  equal to one. This represents a single previous cycle to the PDD displacement, and corresponds to initial loading towards a reduced-strength point halfway between the primary and secondary curves at the PDD displacement (Figure 6-28).

For the other degrading models, strength reduction is considered possible only for PDDs greater than zero.

The parameter RSR is used to describe strength degradation in the context of the Takeda Pinching models and strength reduction in the context of the other degrading models. For this study, values of RSR were arbitrarily set at 100%, 80%, and 60%.

Oscillators were referenced by their initial, undamaged vibration periods, determined using the yield-point secant stiffness, regardless of strength loss and PDDs. Note that changes in strength further affect the initial stiffness of the damaged oscillators.

While the values of the parameters used to model Type A, B, and C behaviors, as well as the hysteresis rules themselves, were chosen somewhat arbitrarily, they were believed to be sufficiently representative to allow meaningful conclusions to be made regarding the effects of prior damage on response characteristics of various wall structures. Values of RSR and PDD were selected to identify trends in response characteristics, not to represent specific structures.

### 6.3.7 Summary of Dynamic Analysis Parameters

Nonlinear dynamic analyses were conducted for SDOF systems using various force/displacement models, various initial strength values, and for various degrees of damage. The analyses were repeated for the 18 selected ground-motion records. The analysis procedures are summarized below.

1. Initially-undamaged oscillators were established at eleven initial periods of vibration, equal to 0.1, 0.2, 0.3, 0.4, 0.5, 0.6, 0.8, 1.0, 1.2, 1.5, and 2.0 seconds. At these periods, the strength necessary to obtain design displacement ductilities (DDD) of 1 (elastic), 2, 4, and 8 were obtained using the bilinear model for each earthquake. This procedure establishes 44 oscillators for each of 18 ground motions.
2. The responses of the oscillators designed in step 1 were computed using the three degrading models (Takeda5, Takeda10, and TakPinch). The yield strength of the degrading oscillators in this step is identical to that determined in the previous step for the bilinear model. The period of vibration of the degrading oscillators, when based on the yield-point secant stiffness, matches that determined in the previous step for the bilinear model.
3. Damage is accounted for by assuming that the force/displacement curves of the oscillators are altered as a result of previous inelastic response. The extent of prior damage is parameterized by PDD. For some cases, the strength of the oscillators is reduced as well. Each of the initially-undamaged, degrading oscillators was considered to have experienced a PDD equal to 1, 2, 4, or 8, but not in excess of the ductility demand for which the oscilla-

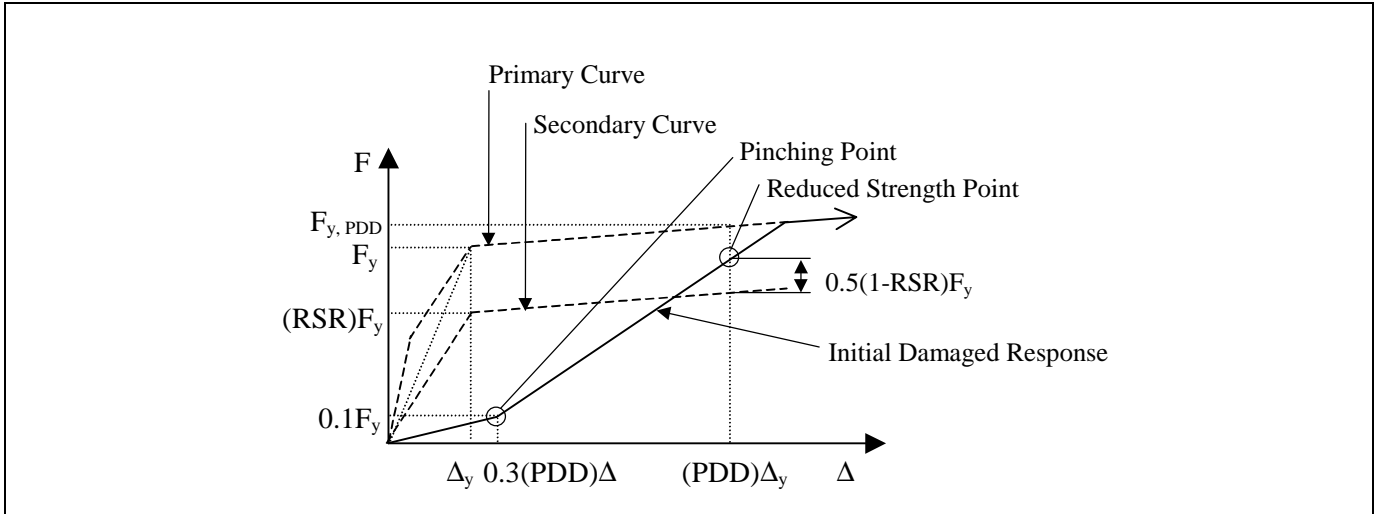


Figure 6-28 Construction of Initial Force-Displacement Response for  $PDD > 0$  and  $RSR < 1$  for Takeda Pinching Model

tor was designed. The effects of cracking on response were determined by considering a PDD of one. Where larger PDDs are considered, reductions in the initial loading and unloading stiffness were determined in accordance with the Takeda model.

4. Strength degradation was modeled explicitly in the TakPinch model. In the Takeda5 and Takeda10 models, strength degradation was approximated by reducing the initial strength of the damaged Takeda5 and Takeda10 models. RSRs equal to 100%, 80%, and 60% were considered. Although the strength reduction considered in the Takeda 5 and Takeda10 models does not model the evolution of strength loss, it suggests an upper bound for the effect of strength degradation on response characteristics.

### 6.3.8 Implementation of Analyses

Over 22,000 inelastic SDOF analyses were conducted using a variety of software programs. The strength of the oscillators was determined using constant-ductility iterations for the bilinear oscillators using the program PCNSPEC (Boroschek, 1991), a modified version of NONSPEC (Mahin and Lin, 1983). Response of the Takeda models was computed using a program developed by Otani (1981). This program was modified at the University of Illinois to include the effects of PDD, pinching, and strength degradation and to identify collapse states for models with negative post-yield stiffness.

## 6.4 Results Of Dynamic Analyses

### 6.4.1 Overview and Nomenclature

This section describes results obtained from the dynamic analyses. Section 6.4.2 characterizes the ground motions in terms of strength and displacement demand characteristics for bilinear oscillators, in order to establish that the ground motions and procedures used give results consistent with previous studies. Section 6.4.3 discusses the response of the Takeda models in some detail, for selected values of parameters. Section 6.4.4 presents summary response statistics for the Takeda models for a broader range of parameter values.

Several identifiers are used in the plots, as follows:

Records:

- SD= Short-duration ground motions.
- LD= Long-duration ground motions.
- FD= Forward-directivity ground motions.

DDD: Design Displacement Ductility. Strength was determined to achieve the specified DDD response for bilinear oscillators having post-yield stiffness equal to 5% of the initial stiffness. Values range from 1 to 8.

PDD: Prior Ductility Demand. This represents a modification of loading and unloading stiffness, to simulate damage caused by

previous earthquakes. Values range from 1 to 8, but not in excess of DDD.

**RSR:** Reduced Strength Ratio. This represents a reduction or degradation of strength and associated changes in stiffness. Values range from 100% to 60%, as detailed in Figures 6-26, 6-27, and 6-28.

**Displacements:**

$d_d$  = Peak displacement response of undamaged oscillator

$d'_d$  = Peak displacement response of damaged oscillator

$d_e$  = Peak displacement response of elastic oscillator having stiffness equal to the yield-point secant stiffness of the corresponding Takeda oscillator

Space constraints limit the number of included figures. Selected results for oscillators designed for a displacement ductility of 8 are presented below. Elastic response characteristics are presented as part of the ground motion plots in Figures 6-2 to 6-19.

### 6.4.2 Response of Bilinear Models

Figures 6-29 to 6-31 present the response of bilinear models to the SD, LD, and FD ground motions, respectively. The ratio of peak displacement of the inelastic model to the peak displacement response of an elastic oscillator having the same initial period,  $d_d/d_e$ , is presented in the upper plot of each figure. The lower plot presents the ratio of elastic strength demand to the yield strength provided in order to attain the specified DDD, which in this case equals 8.

When the strength reduction factor,  $R$ , has a value of 8, the inelastic design strength is 1/8 of the elastic strength. For DDD = 8, an  $R = 8$  means that the reduced inelastic design strength and the resulting oscillator ductility are equal. If  $R$  is greater than 8, say 12, for DDD = 8, then the reduced inelastic design strength of the structure can be 1/12 of the expected elastic strength to achieve an oscillator ductility of 8. That is, for any  $R$ , the structure can be designed for 1/ $R$  times the elastic needed strength to achieve a ductility of DDD.

Response to each ground motion is indicated by the plotted symbols, which are ordered by increasing characteristic period,  $T_g$ . It was found that the displacement and strength data are better organized when plotted against the ratio  $T/T_g$  instead of the reference period,  $T$ . The plots present data only for

$T/T_g < 4$  in order to reveal sufficient detail in the range  $T/T_g < 1$ .

The trends shown in Figures 6-29 through 6-31 resemble those reported by other researchers, for example, Shimazaki and Sozen (1984), Miranda (1991), and Nassar and Krawinkler (1991). However, it can be observed that the longer-period structures subjected to ground motions with forward-directivity effects show a peak displacement response in the range of approximately 0.5 to 2 times the elastic structure response, somewhat in excess of values typical of the other classes of ground motion. Additionally, strength-reduction factors,  $R$ , tend to be somewhat lower for the FD motions, representing the need to supply a greater proportion of the elastic strength demand in order to maintain prespecified DDDs.

### 6.4.3 Response of Takeda Models

The Takeda models were provided with lateral strength equal to that determined to achieve specified DDDs of 1, 2, 4, and 8 for the corresponding bilinear models, based on the yield-point secant stiffness.

Prior damage was parameterized by prior ductility demand (PDD), possibly in conjunction with strength reduction or strength degradation, which is parameterized by RSR. PDD greater than zero (damage present) and RSR less than one (strength reduced or degrading) both cause the initial period of the oscillator to increase. When previous damage has caused displacements in excess of the yield displacement (PDD > 1), even small displacements cause energy dissipation through hysteretic response. No further attention is given to those oscillators for which the imposed PDD exceeds the response of the undamaged oscillator, and these data points are not represented on subsequent plots.

#### 6.4.3.1 Response of the Takeda5 Model

It is of interest to observe how structures proportioned based on the bilinear model respond if their force/displacement response is represented more accurately by a Takeda model. This interest is based in part on the widespread use of the bilinear model in developing current displacement-based design approaches.

Figures 6-32 through 6-34 present the response of Takeda5 models in which the oscillator strength was set to achieve a bilinear displacement ductility demand of 8. The upper plot of each figure shows the ratio of peak displacement response to the peak response of an elastic

(Text continued on page 134)

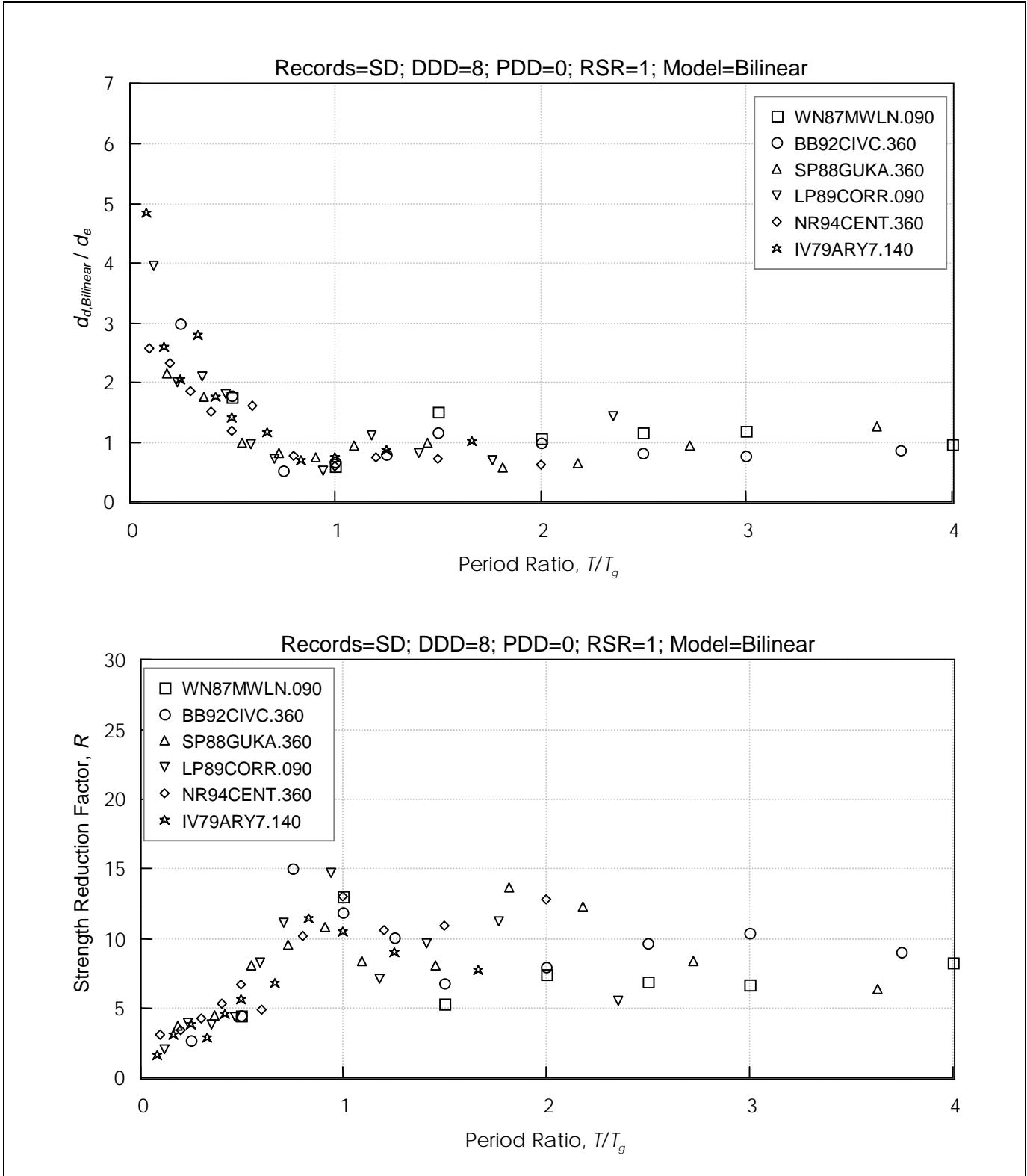


**Figure 6-29** Response of Bilinear Oscillators to Short Duration Records (DDD= 8)  
 DDD = Design Displacement Ductility; PDD = Prior Ductility Demand; RSR = Reduced Strength Ratio

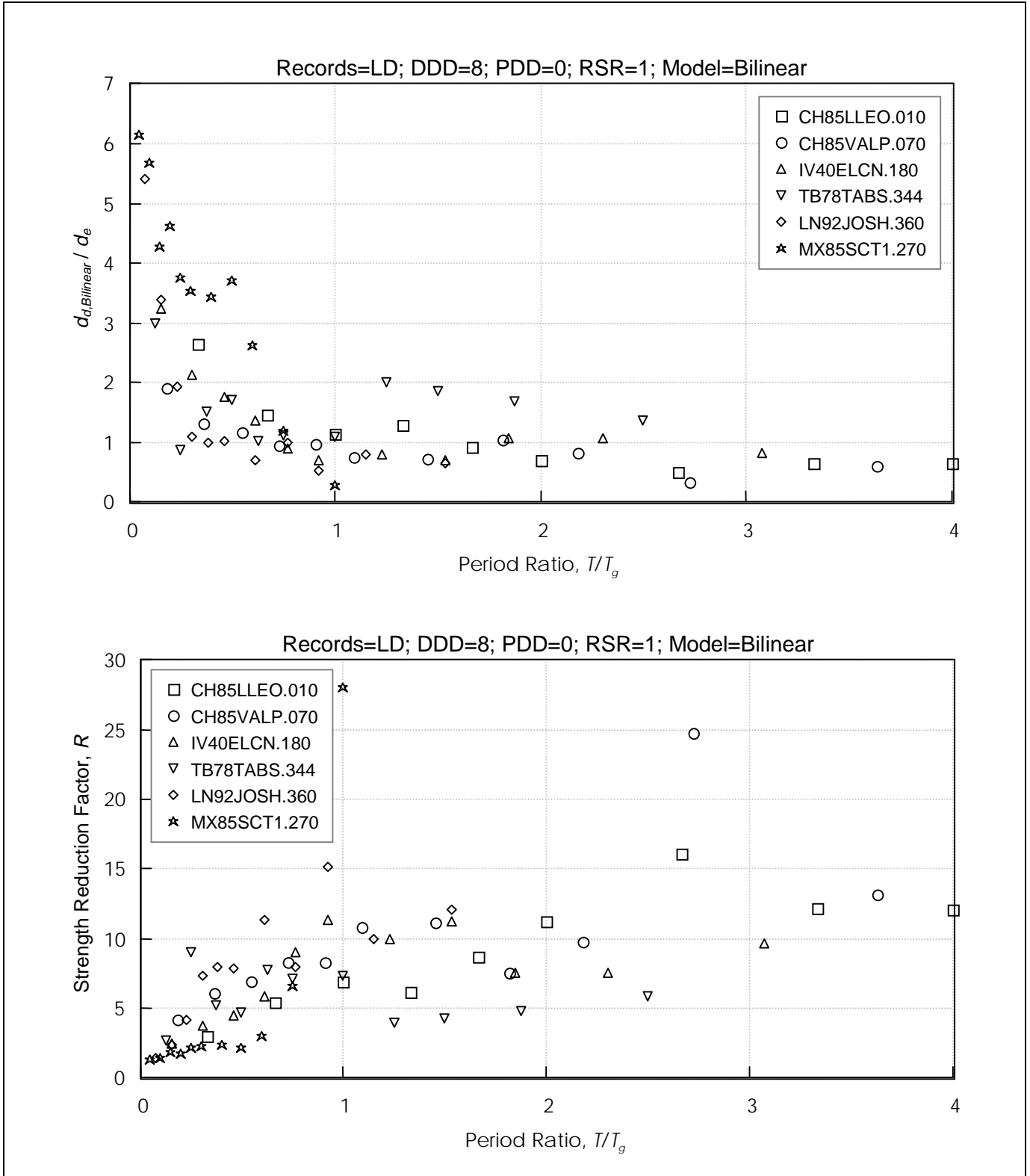
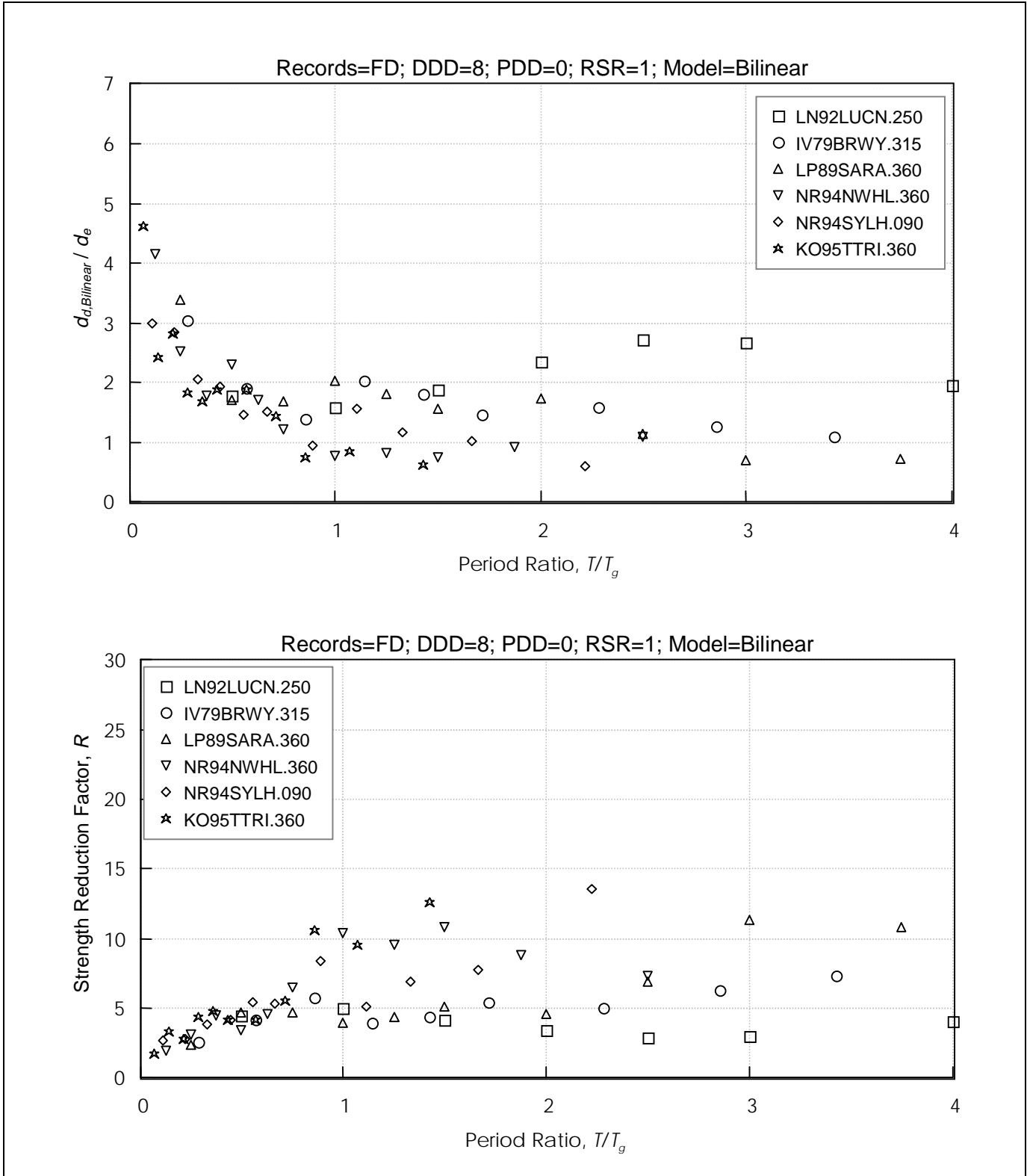
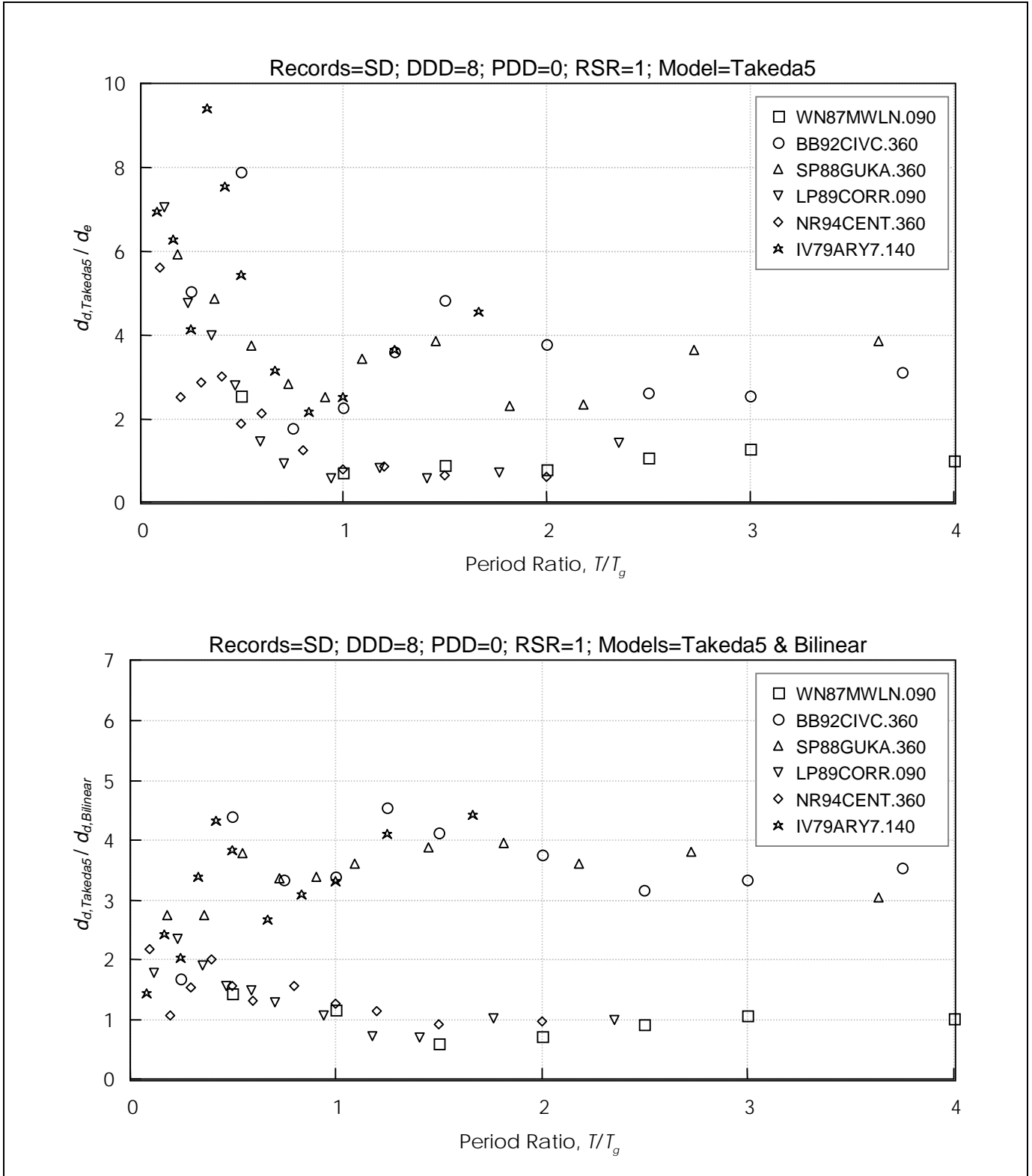


Figure 6-30 Response of Bilinear Oscillators to Long Duration Records (DDD= 8)  
 DDD = Design Displacement Ductility; PDD = Prior Ductility Demand; RSR = Reduced Strength Ratio



**Figure 6-31** Response of Bilinear Oscillators to Forward Directive Records (DDD= 8)  
 DDD = Design Displacement Ductility; PDD = Prior Ductility Demand; RSR = Reduced Strength Ratio



**Figure 6-32** Displacement Response of Takeda Models Compared with Elastic Response and Bilinear Response, for Short-Duration Records (DDD= 8 and RSR= 1)  
 DDD = Design Displacement Ductility; PDD = Prior Ductility Demand; RSR = Reduced Strength Ratio

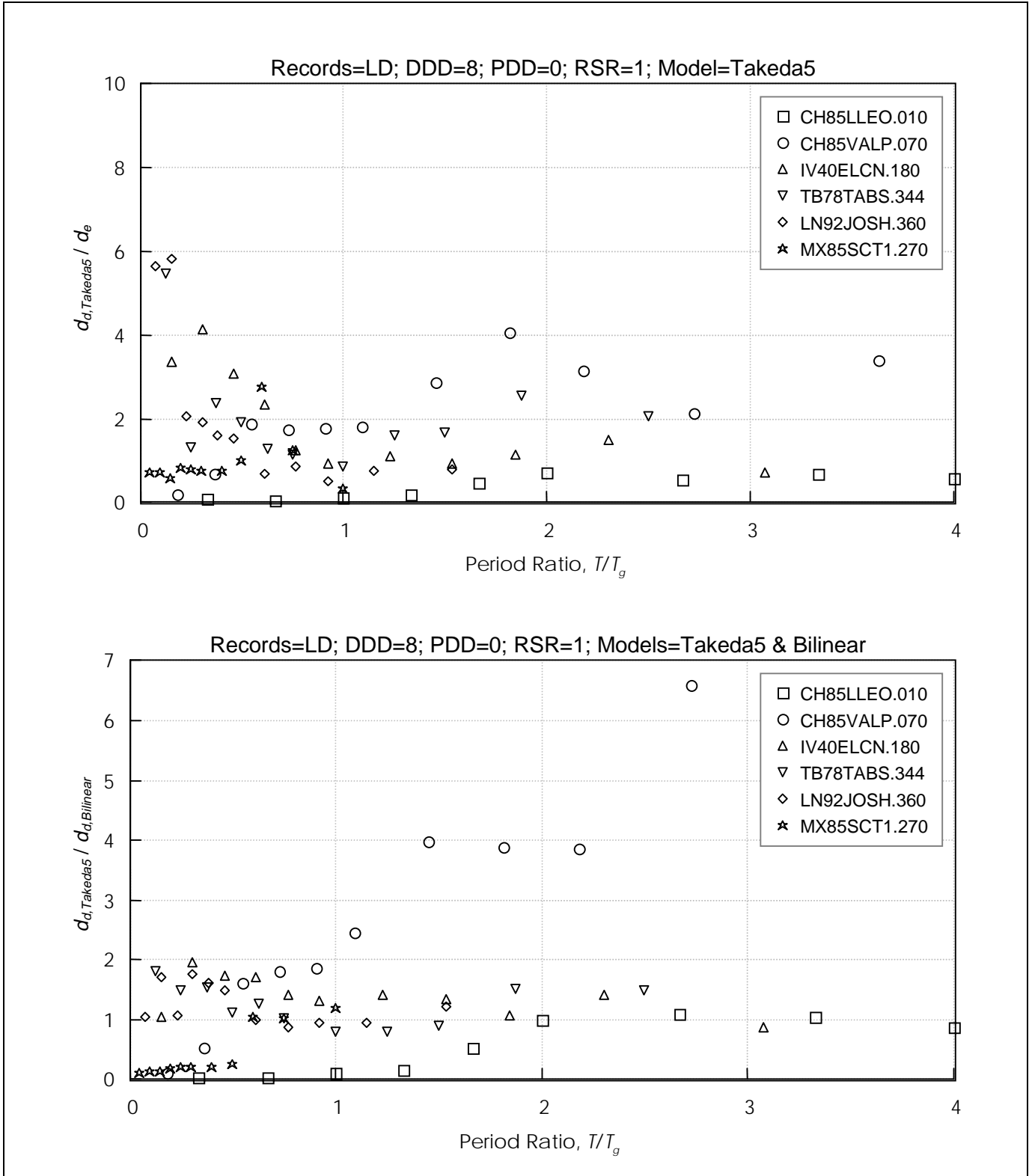


**Figure 6-33** Displacement Response of Takeda Models Compared with Elastic Response and Bilinear Response for Long-Duration Records (DDD= 8 and RSR= 1)  
 DDD = Design Displacement Ductility; PDD = Prior Ductility Demand; RSR = Reduced Strength Ratio

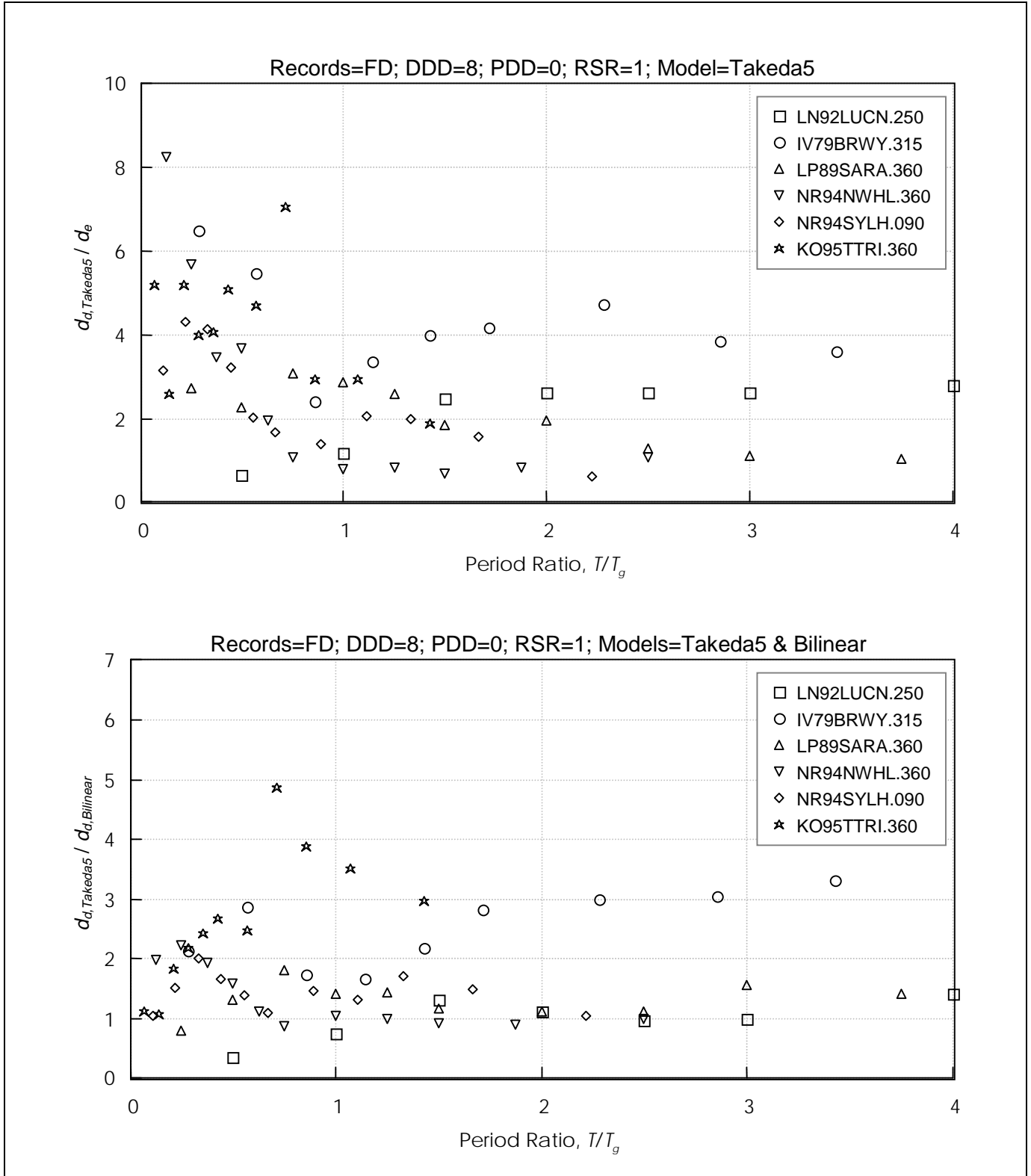


**Figure 6-34** Displacement Response of Takeda Models Compared with Elastic Response and Bilinear Response for Forward Directive Records (DDD= 8 and RSR= 1)  
 DDD = Design Displacement Ductility; PDD = Prior Ductility Demand; RSR = Reduced Strength Ratio

analog,  $d_d/d_e$ . The upper plots of Figures 6-32 through 6-34 are analogous to those presented in Figures 6-29 through 6-31.

The lower plots of Figures 6-32 through 6-34 show the ratio of the Takeda5 and bilinear ultimate displacements,  $d_{d,Takeda5}/d_{d,Bilinear}$ . It is clear that peak displacements of the Takeda model may be several times larger or smaller than those obtained with the corresponding bilinear model.

The effect of damage on the Takeda5 model is shown in Figures 6-35 through 6-40, for Takeda5 oscillators that were initially designed for a bilinear DDD of 8. The upper plot of each figure shows the response without strength reduction (RSR = 1); the lower plot shows response for RSR = 0.6.

Figures 6-35 through 6-37 show the effect of cracking on response. The displacement response,  $d'_d$ , of Takeda5 oscillators subjected to a PDD of one is compared with the response of the corresponding undamaged Takeda5 oscillators,  $d_d$ . Where no strength degradation occurs (RSR = 1), cracking rarely causes an increase in displacement demand; for the vast majority of oscillators, cracking is observed to cause a slight decrease in the peak displacement response. Reductions in strength typically cause a noticeable increase in displacement response, particularly for low  $T/T_g$ .

Figures 6-38 through 6-40 show the effect of a PDD of 8 on peak displacement,  $d'_d$ , relative to the response of the corresponding undamaged oscillators. Prior damage is observed to cause modest changes in displacement response where the strength is maintained (RSR = 1); displacements may increase or decrease. Where displacements increase, they rarely increase more than about 10% above the displacement of the undamaged oscillator for the short-duration and long-duration motions. For the forward directivity motions, they rarely increase more than about 30% above the displacement of the undamaged oscillator. The largest displacements tend to occur more frequently for  $T < T_g$ .

The above discussion concerned oscillators for which the strength is maintained. When strength is reduced (RSR = 0.6), prior ductility demand may cause displacements to increase or decrease, but the tendency for displacements to increase is more prominent than for RSR = 1. Furthermore, the increase in displacement tends to be larger than for RSR = 1. Reduction in strength, as represented in Figure 6-26, also causes

reduction in stiffness, and both effects contribute to the tendency for displacements to increase.

To understand the effects of prior damage on the response of the Takeda5 models, it is helpful to consider several oscillators exposed to the IV40ELCN.180 (El Centro) record. Figures 6-41 to 6-45 plot the response of oscillators having initial (reference) periods of 0.2, 0.5, 1.0, 1.5, and 2.0 sec, respectively, to this ground motion. The oscillators have yield strength equal to that required to obtain displacement ductility demands of 8 for the bilinear model. Oscillators having PDD of 0 (undamaged), 1, 4, and 8 are considered. Displacement time-histories (40 sec) of the oscillators are plotted at the top of each figure. Details of the first 10 seconds of response are shown below these. The solid lines represent the response of the initially-undamaged oscillators, and the dashed and dotted lines represent oscillators with PDD > 0. Force/displacement plots for the first 10 sec of response of each oscillator are provided in the lower part of the figure, using the same PDD legend. It can be observed that even though the undamaged oscillators initially have greater stiffness, their displacement response tends to converge upon the response of the initially-damaged oscillators within a few seconds. The displacement response of the damaged oscillators tends to be in phase with that of the initially-undamaged oscillators, and maximum values tend to be similar to and to occur at approximately the same time as the undamaged oscillator peaks. Thus, it appears that prior ductility demands have only a small effect on oscillator response characteristics and do not cause a fundamentally different response to develop.

#### 6.4.3.2 Response of the TakPinch Model

Figures 6-46 to 6-48 plot the ratio,  $d'_d/d_d$ , of damaged and undamaged displacement response for the TakPinch models having DDD = 8 and PDD = 8, for RSR = 1 and 0.6. Figure 6-49 plots the displacement time-history of TakPinch oscillators subjected to the NS component of the 1940 El Centro record, and Figure 6-50 plots results for oscillators having cyclic strength degradation given by RSR = 0.6. These oscillators have a reference period of one second, DDD = 8, and various PDDs.

By comparison with the analogous figures for the Takeda5 model (Figures 6-38 to 6-40 and 6-43), it can be observed that: (1) for RSR = 1 (no strength degradation), the effect of PDD on displacement response is typically small for the Takeda5 and TakPinch oscillators, and (2) the effect of cyclic strength degradation, as implemented here, is also relatively small. Thus, the observation that prior

(Text continued on page 151)

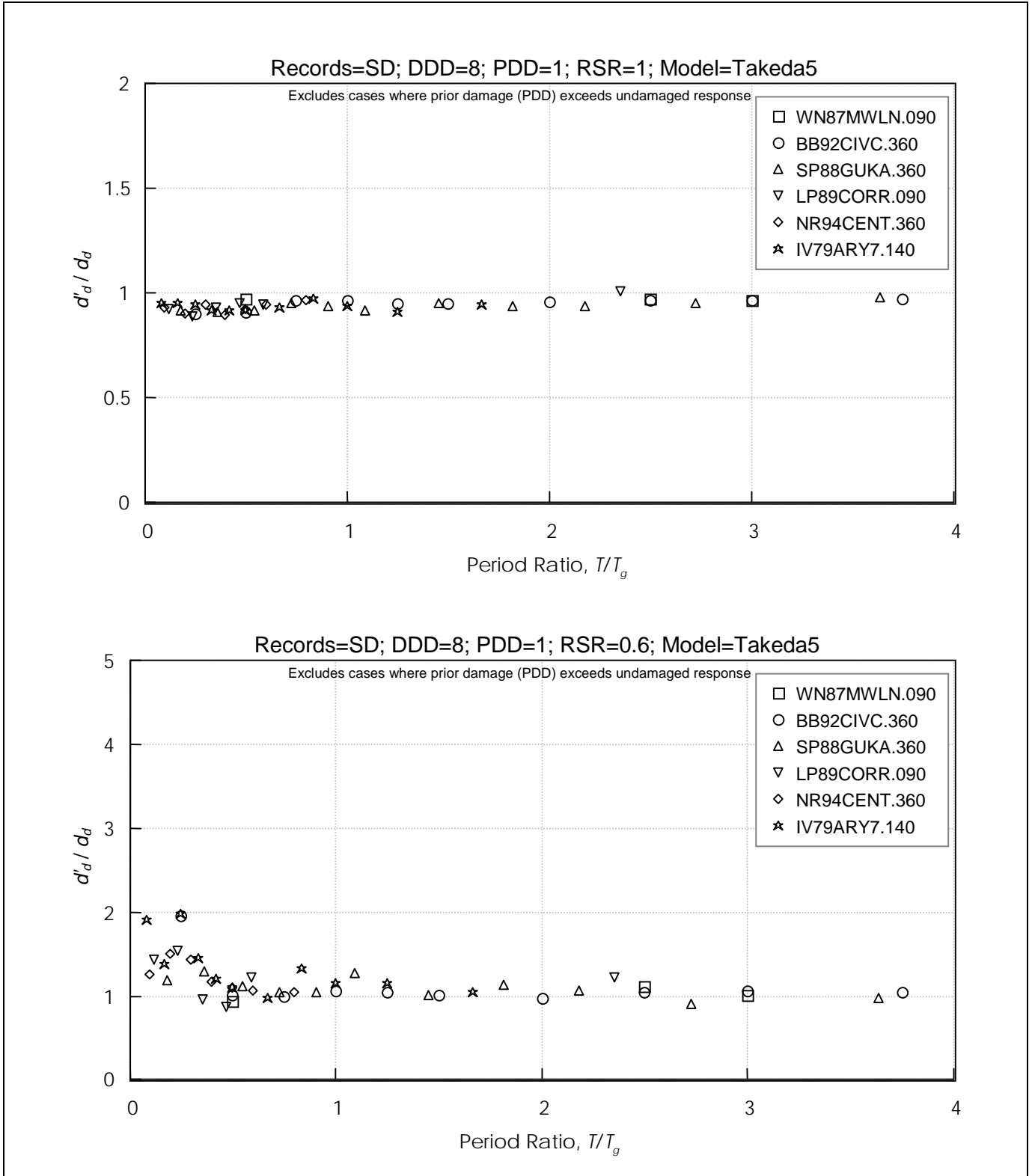


**Figure 6-35** Effect of Cracking Without and With Strength Reduction on Displacement Response of Takeda5 Models, for Short-Duration Records (DDD= 8 and PDD= 1)  
 DDD = Design Displacement Ductility; PDD = Prior Ductility Demand; RSR = Reduced Strength Ratio

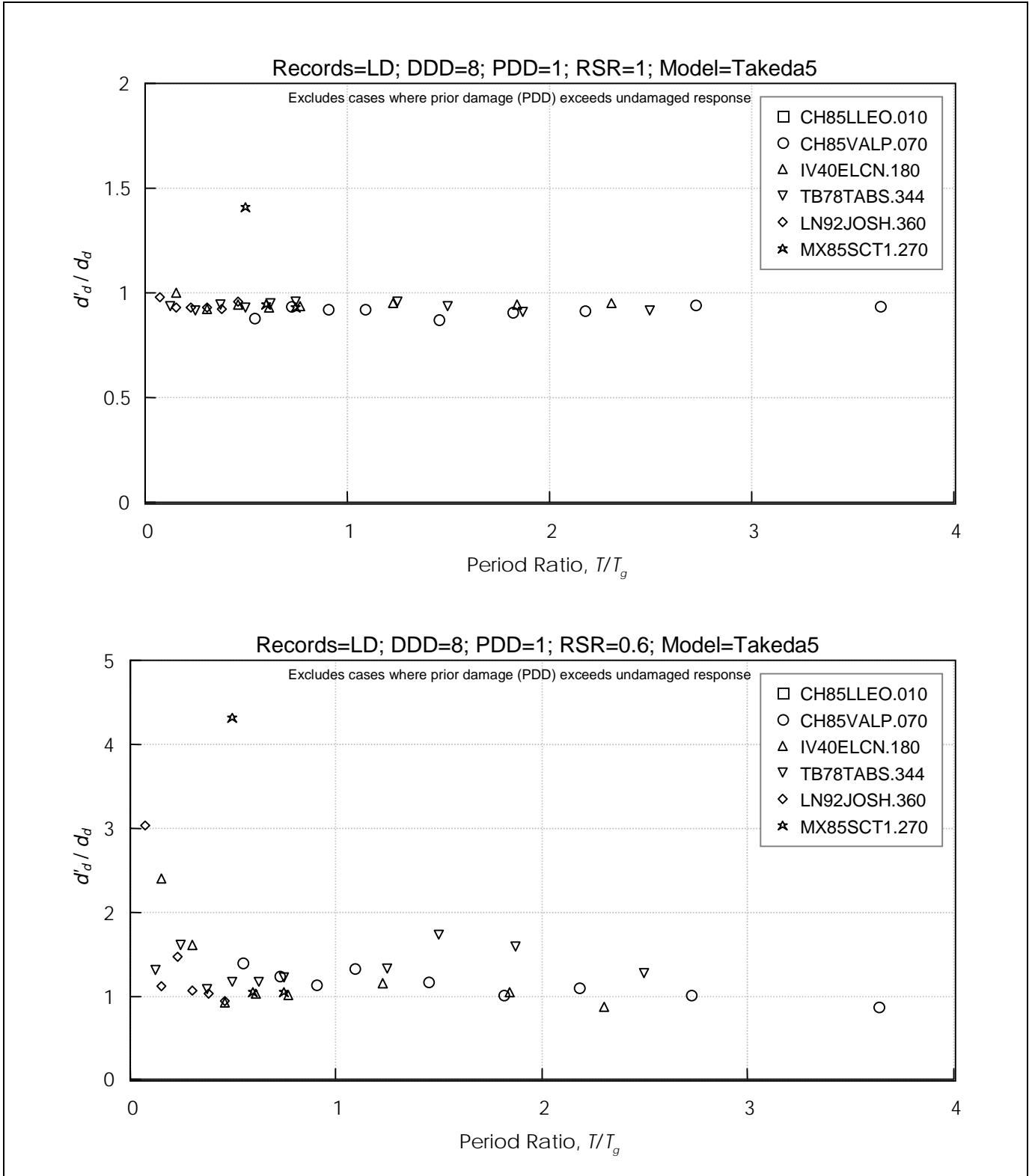


**Figure 6-36** Effect of Cracking Without and With Strength Reduction on Displacement Response of Takeda5 Models, for Long-Duration Records (DDD= 8 and PDD= 1)  
 DDD = Design Displacement Ductility; PDD = Prior Ductility Demand; RSR = Reduced Strength Ratio

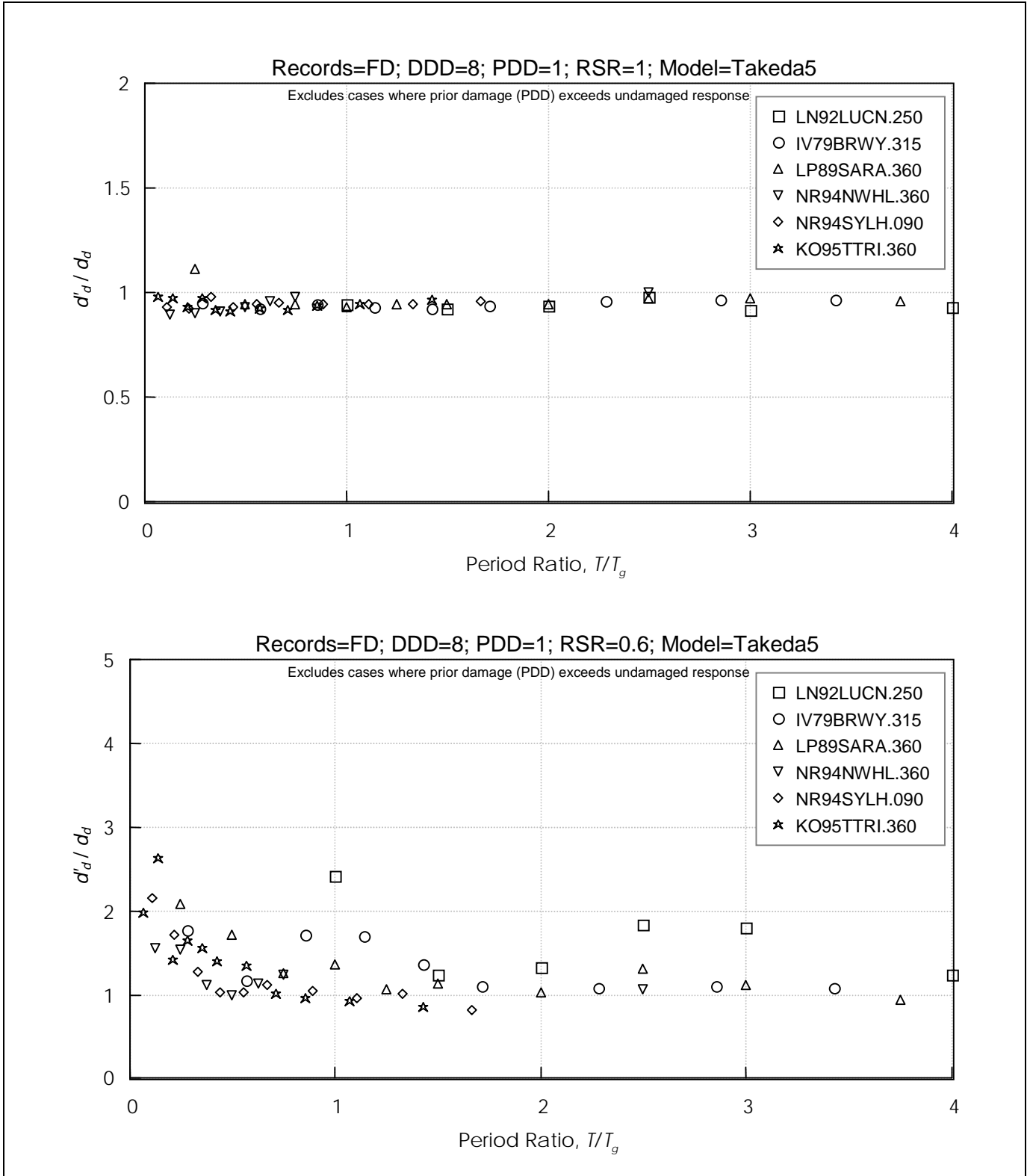


**Figure 6-37** Effect of Cracking Without and With Strength Reduction on Displacement Response of Takeda5 Models, for Forward Directive Records (DDD= 8 and PDD= 1)  
 DDD = Design Displacement Ductility; PDD = Prior Ductility Demand; RSR = Reduced Strength Ratio

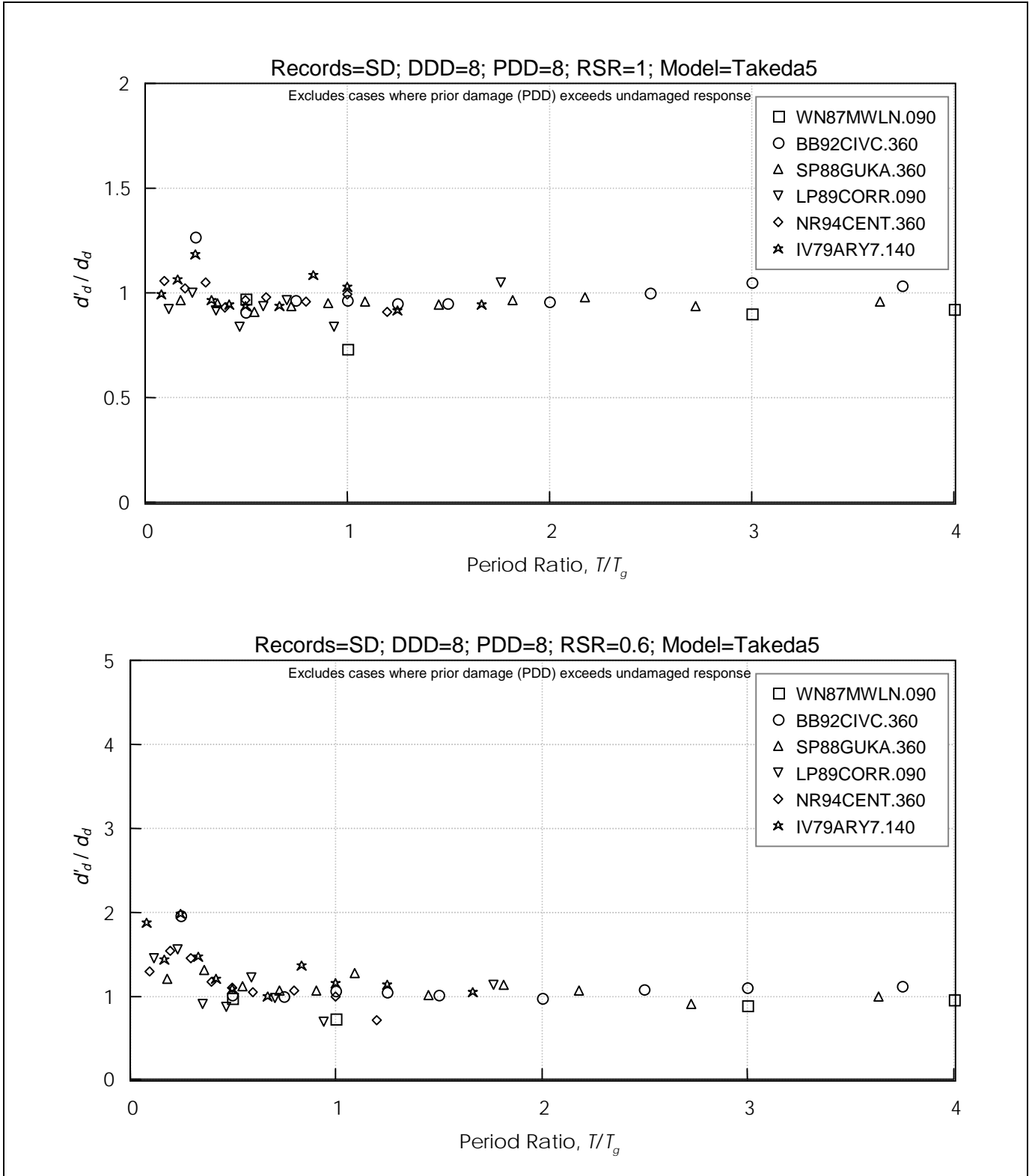


**Figure 6-38** Effect of Large Prior Ductility Demand Without and With Strength Reduction on Displacement Response of Takeda5 Models, for Short Duration Records (DDD= 8 and PDD= 8)  
 DDD = Design Displacement Ductility; PDD = Prior Ductility Demand; RSR = Reduced Strength Ratio

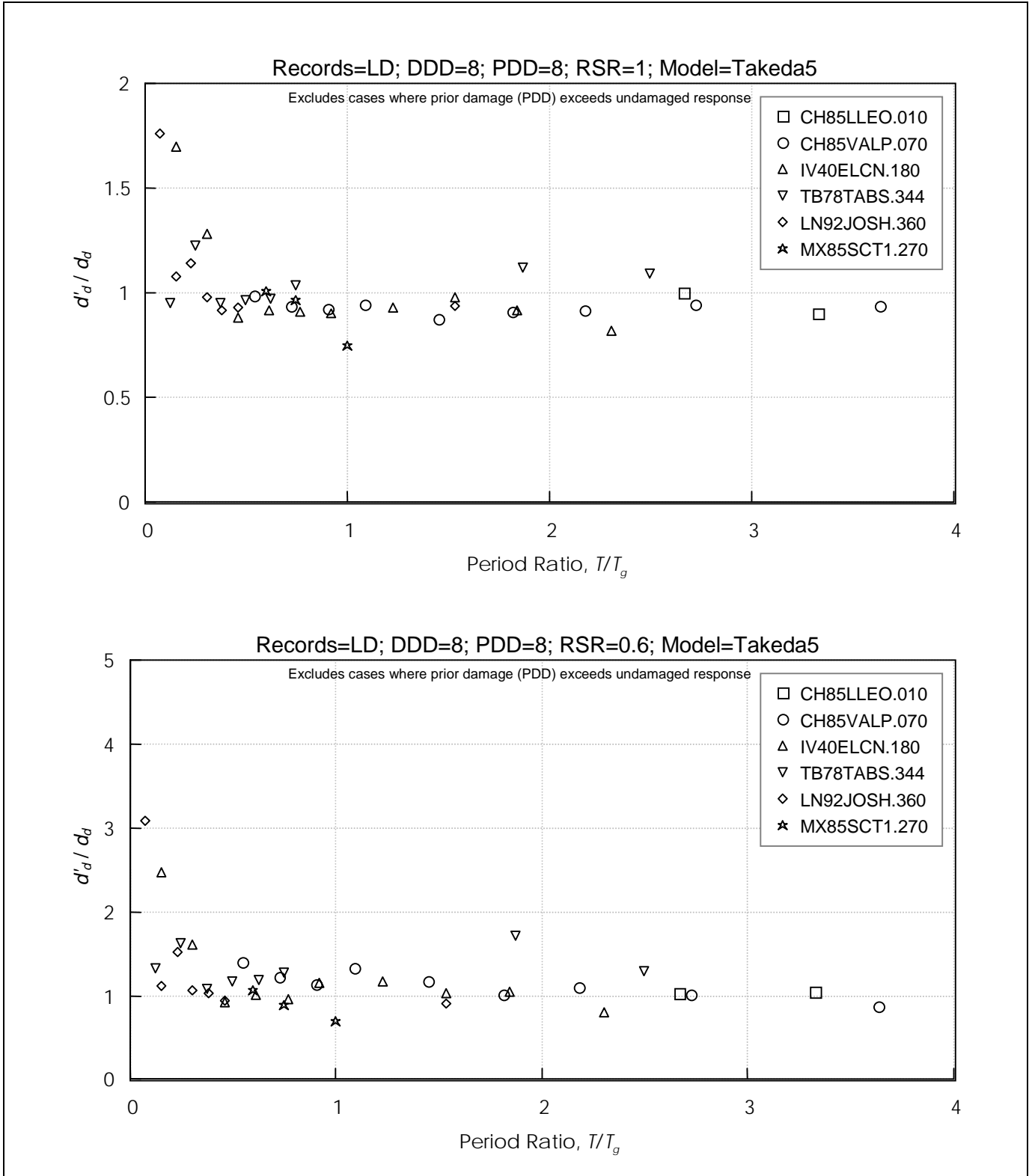


**Figure 6-39** Effect of Large Prior Ductility Demand Without and With Strength Reduction on Displacement Response of Takeda5 Models, for Long Duration Records (DDD = 8 and PDD = 8)  
 DDD = Design Displacement Ductility; PDD = Prior Ductility Demand; RSR = Reduced Strength Ratio

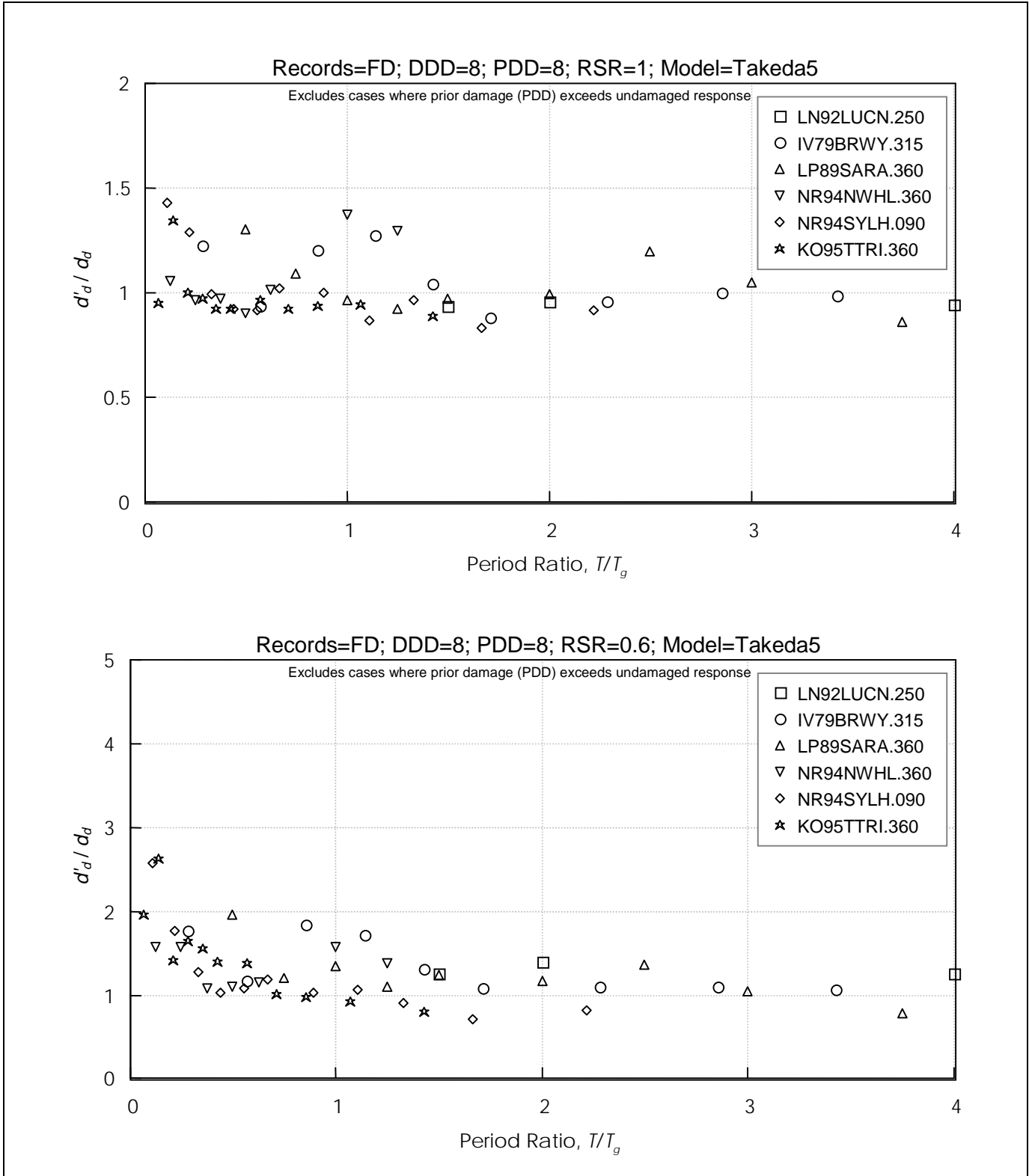


**Figure 6-40** Effect of Large Prior Ductility Demand Without and With Strength Reduction on Displacement Response of Takeda5 Models, for Forward Directive Records (DDD= 8 and PDD= 8)  
 DDD = Design Displacement Ductility; PDD = Prior Ductility Demand; RSR = Reduced Strength Ratio

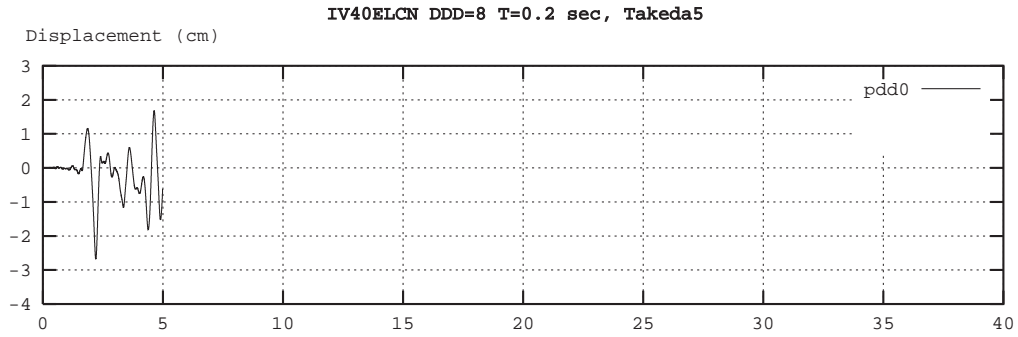


Figure 6-41 Effect of Damage on Response to El Centro (IV40ELCN.180) for Takeda5, T=0.2 sec (DDD= 8)  
DDD = Design Displacement Ductility

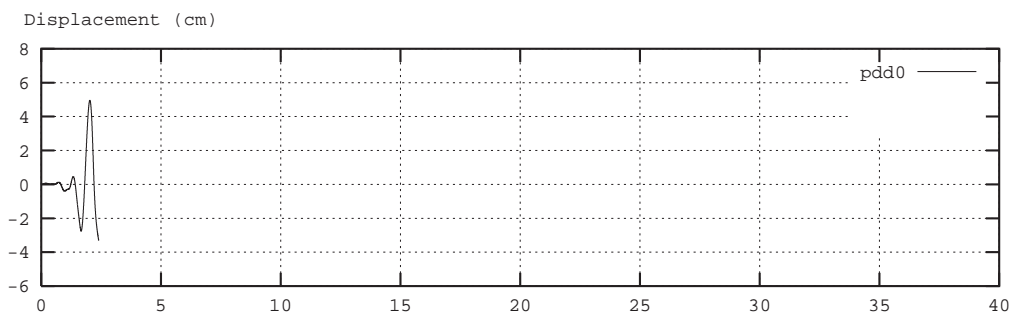


Figure 6-42 Effect of Damage on Response to El Centro (IV40ELCN.180) for Takeda5,  $T=0.5$  sec (DDD= 8)  
DDD = Design Displacement Ductility

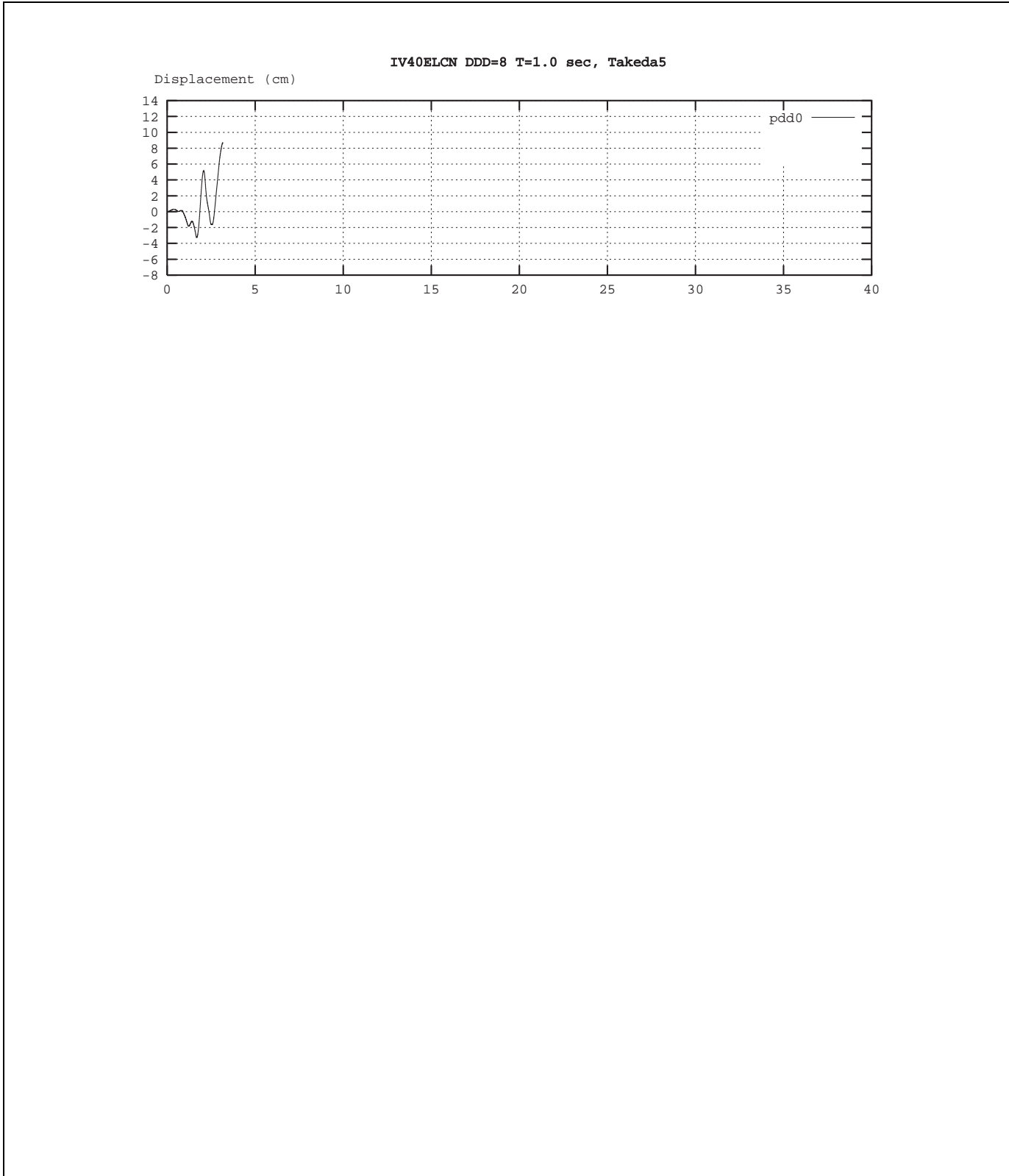


Figure 6-43 Effect of Damage on Response to El Centro (IV40ELCN.180) for Takeda5, T=1.0 sec (DDD= 8)  
DDD = Design Displacement Ductility

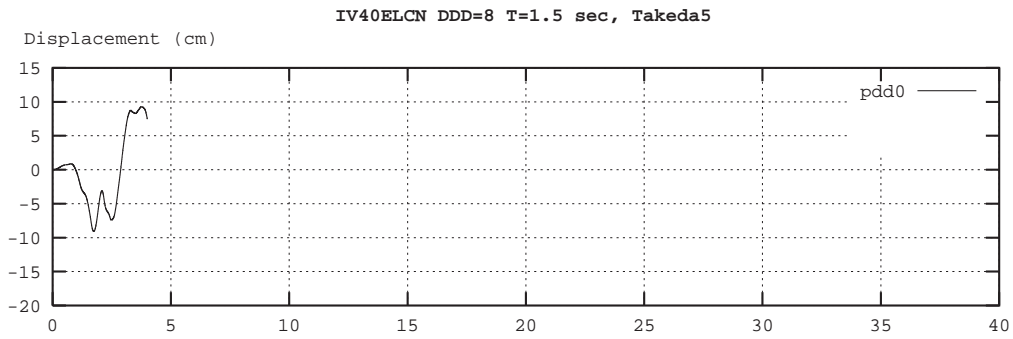


Figure 6-44 Effect of Damage on Response to El Centro (IV40ELCN.180) for Takeda5, T=1.5 sec (DDD= 8)  
DDD = Design Displacement Ductility

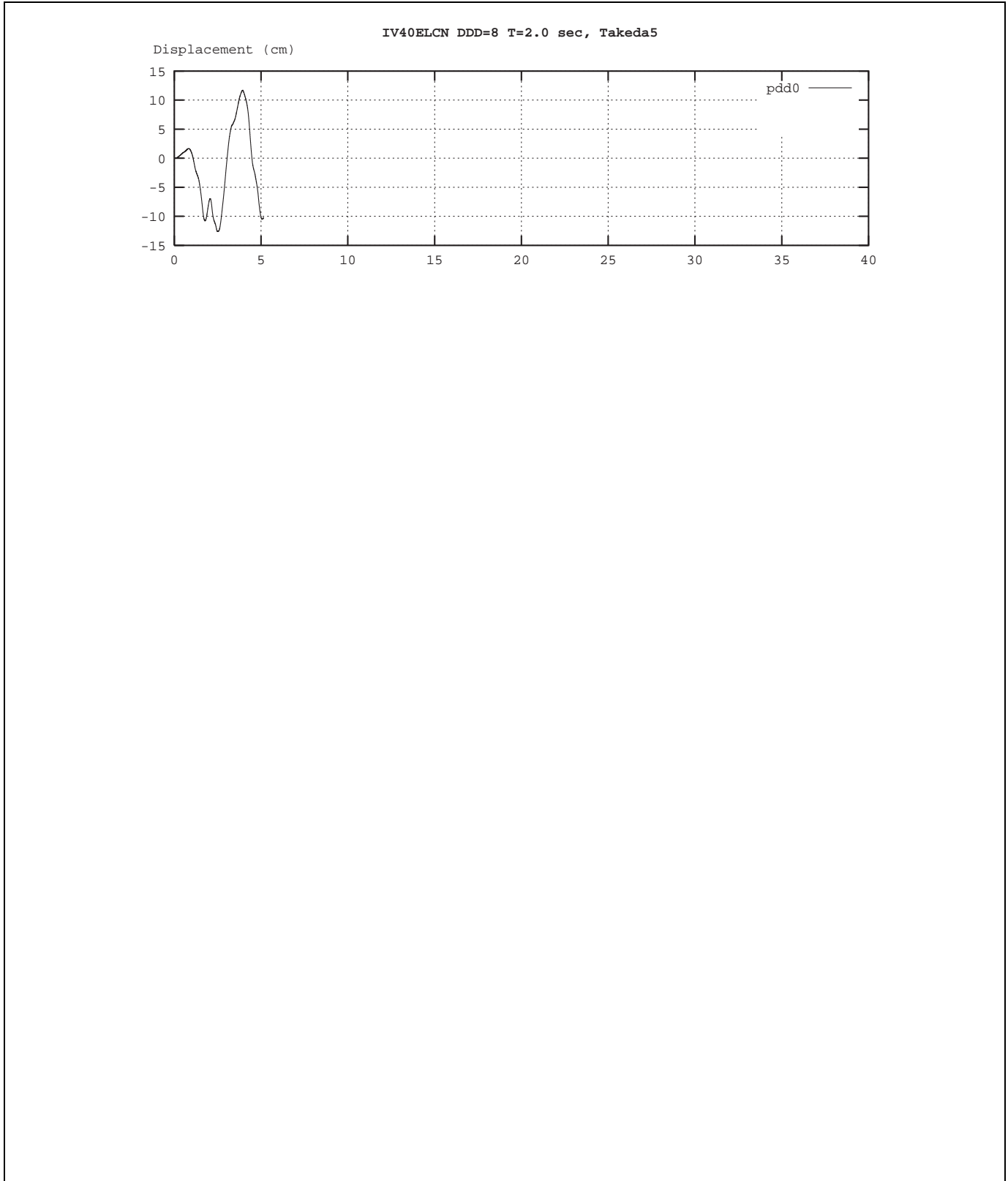
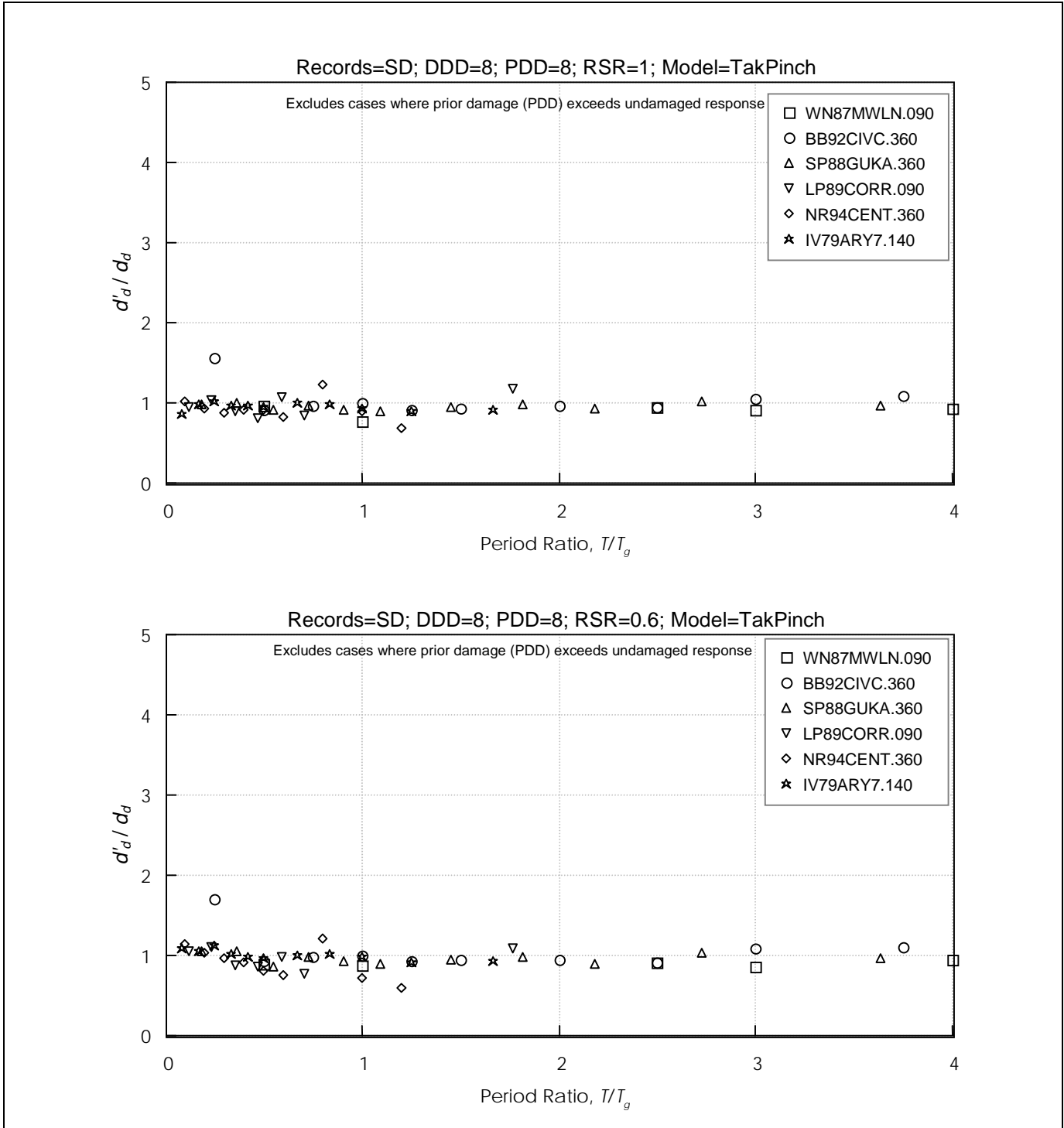
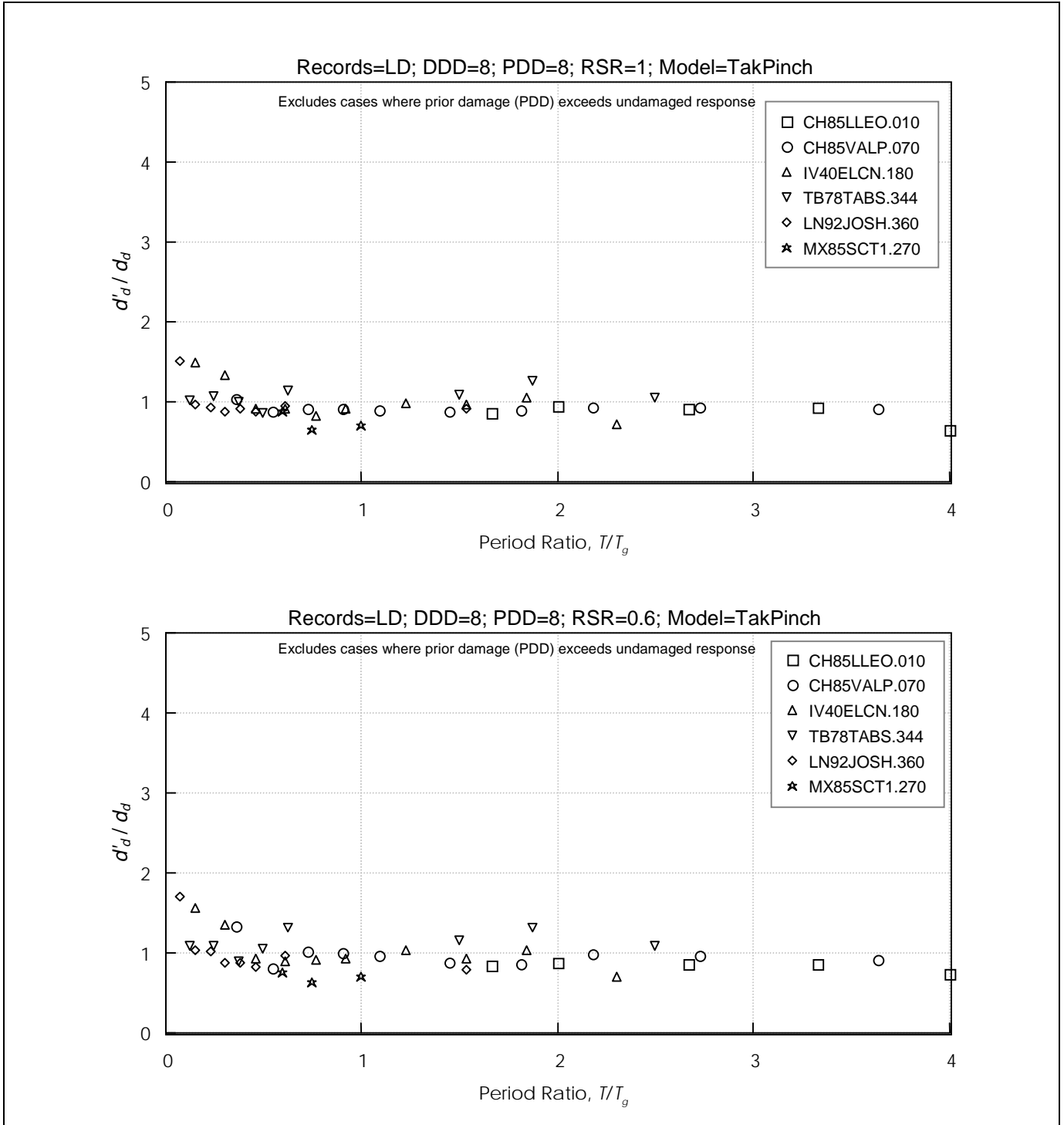


Figure 6-45 Effect of Damage on Response to El Centro (IV40ELCN.180) for Takeda5, T=2.0 sec (DDD= 8)  
DDD = Design Displacement Ductility



**Figure 6-46** Effect of Large Prior Ductility Demand Without and With Strength Reduction on Displacement Response of TakPinch Models, for Short Duration Records (DDD= 8 and PDD= 8)  
 DDD = Design Displacement Ductility; PDD = Prior Ductility Demand; RSR = Reduced Strength Ratio



**Figure 6-47** *Effect of Large Prior Ductility Demand Without and With Strength Reduction on Displacement Response of TakPinch Models, for Long Duration Records (DDD= 8 and PDD= 8)*  
**DDD = Design Displacement Ductility; PDD = Prior Ductility Demand; RSR = Reduced Strength Ratio**

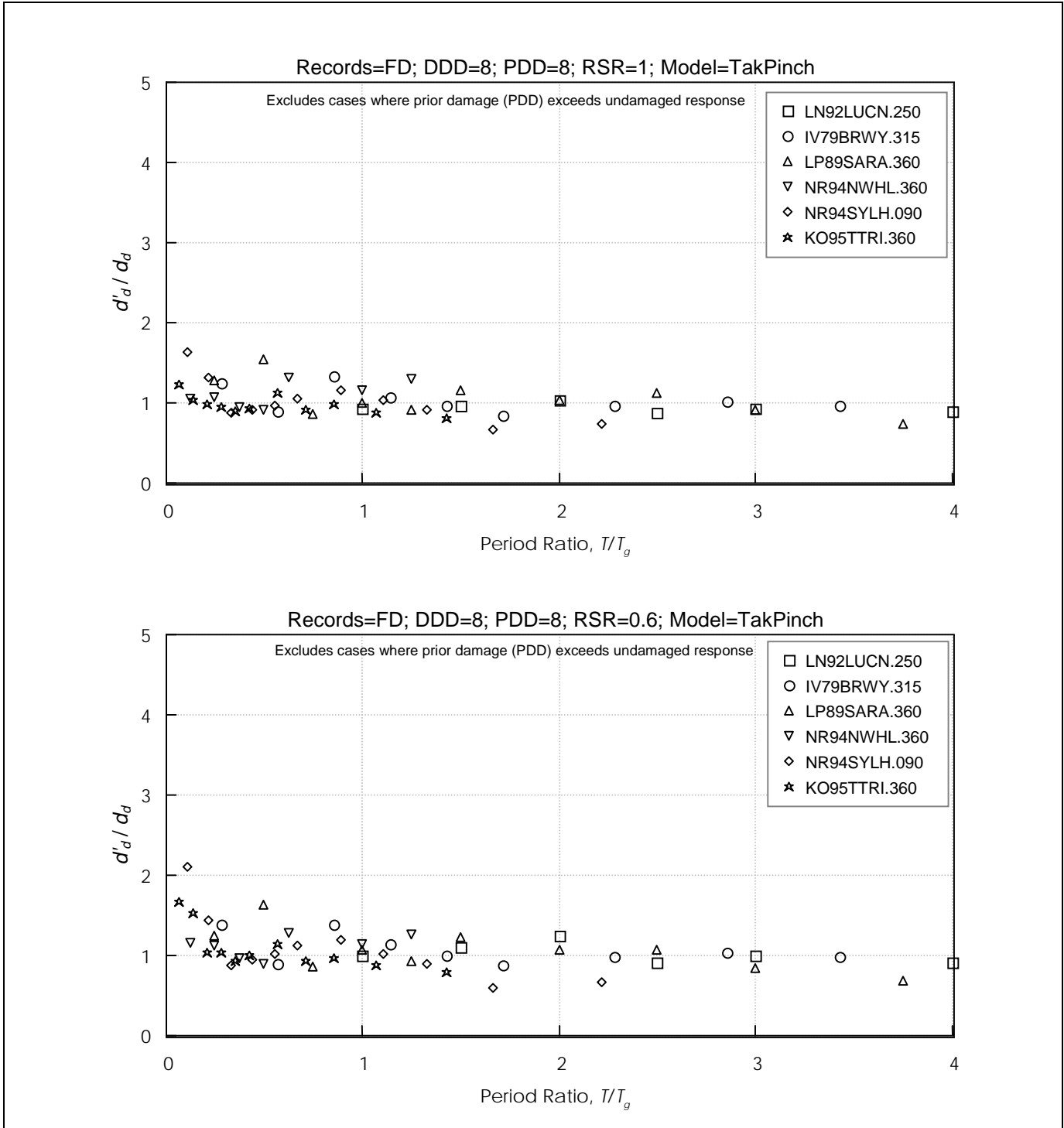


**Figure 6-48** Effect of Large Prior Ductility Demand Without and With Strength Reduction on Displacement Response of TakPinch, for Forward Directive Records (DDD = 8 and PDD = 8)  
 DDD = Design Displacement Ductility; PDD = Prior Ductility Demand; RSR = Reduced Strength Ratio

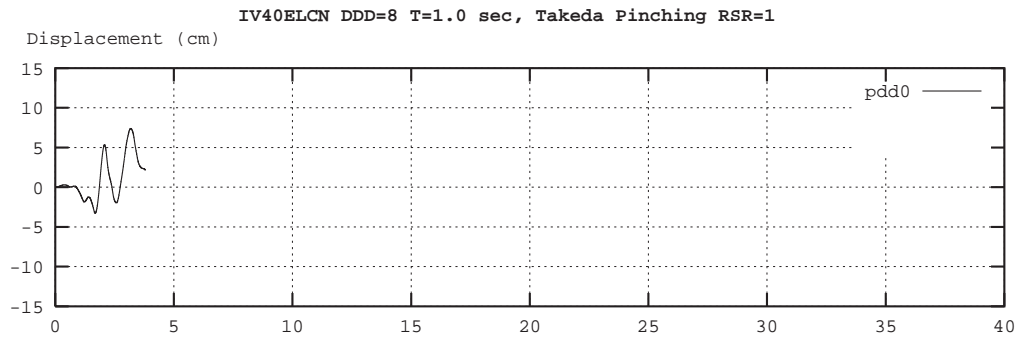
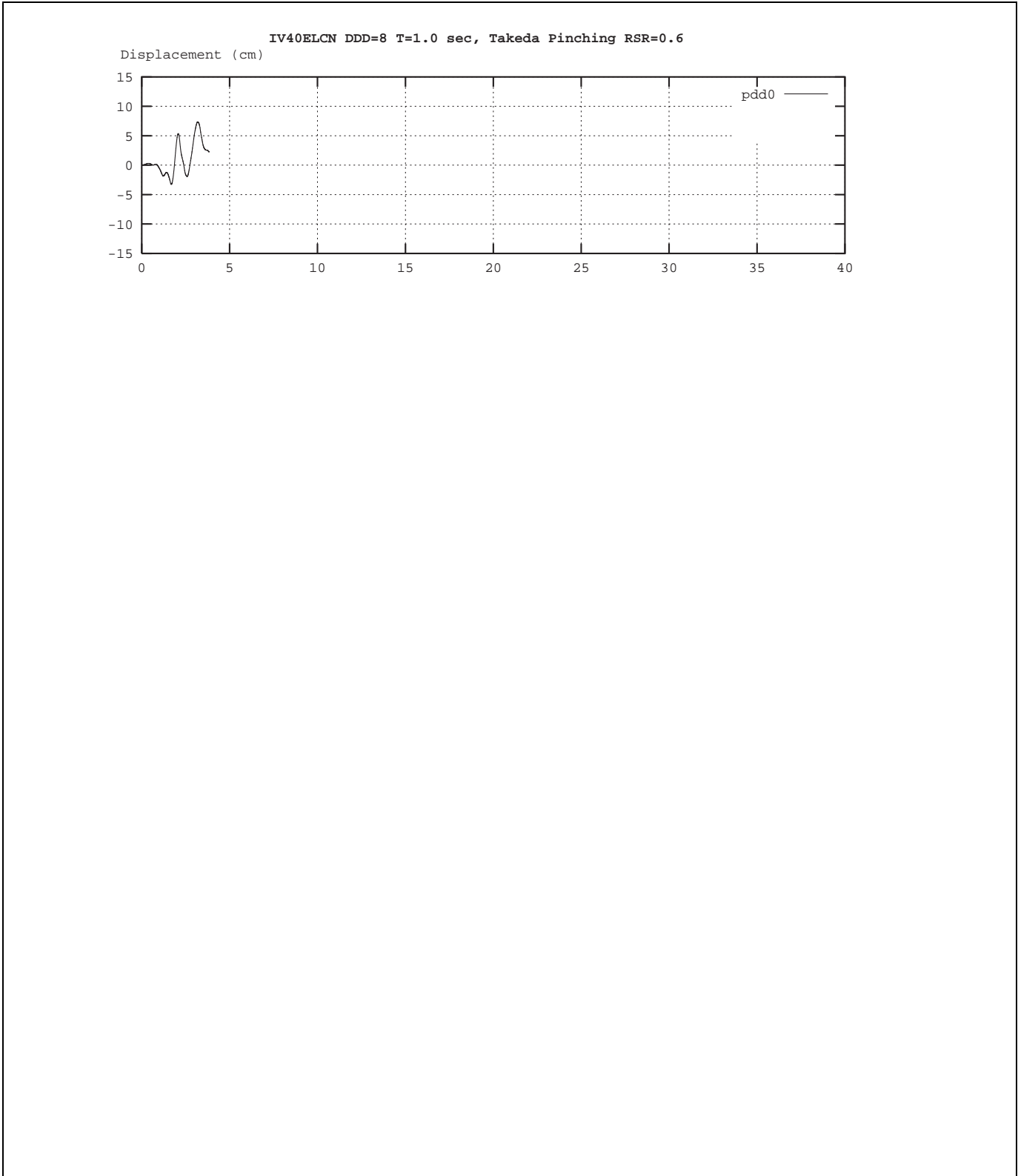


Figure 6-49 Effect of Damage on Response of TakPinch Model to El Centro (IV40ELCN.180) for T=1.0 sec and RSR= 1 (DDD= 8)  
DDD = Design Displacement Ductility



**Figure 6-50** Effect of Damage on Response of TakPinch Model to El Centro (IV40ELCN.180) for T=1.0 sec and RSR = 0.6 (DDD= 8)  
DDD = Design Displacement Ductility